ornl

OAK RIDGE NATIONAL LABORATORY

UNION CARBIDE

NUREG/CR-3243
ORNL/Sub/82-22252/1

Comparisons of ASME Code Fatigue Evaluation Methods for Nuclear Class 1 Piping with Class 2 or 3 Piping

E. C. Rodabaugh

Work Performed for
U.S. Nuclear Regulatory Commission
Office of Nuclear Regulatory Research
under
DOE Interagency Agreement No. 40-550-75

OPERATED BY
UNION CARBIDE CORPORATION
FOR THE UNITED STATES
DEPARTMENT OF ENERGY

ornl

OAK
RIDGE
NATIONAL
LABORATORY

UNION
CARBIDE

NUREG/CR-3243
ORNL/Sub/82-22252/1

Comparisons of ASME Code Fatigue Evaluation Methods for Nuclear Class 1 Piping with Class 2 or 3 Piping

E. C. Rodabaugh

Work Performed for
U.S. Nuclear Regulatory Commission
Office of Nuclear Regulatory Research
under
DOE Interagency Agreement No. 40-550-75

OPERATED BY
UNION CARBIDE CORPORATION
FOR THE UNITED STATES
DEPARTMENT OF ENERGY

Printed in the United States of America. Available from
National Technical Information Service
U.S. Department of Commerce
5285 Port Royal Road, Springfield, Virginia 22161

Available from

CPO Sales Program
Division of Technical Information and Document Control
U.S. Nuclear Regulatory Commission
Washington, D.C. 20555

NUREG/CR-3243

Comparisons of ASME (American Society for Mechanical Engineers) Code Fatigue Evaluation Methods for Nuclear Class 1 Piping with Class 2 or 3 Piping

Oak Ridge National Lab., TN

Prepared for

Nuclear Regulatory Commission, Washington, DC

Jun 83

NUREG/CR-3243
ORNL/Sub/82-22252/1
Dist. Category AN

Engineering Technology Division

COMPARISONS OF ASME CODE FATIGUE EVALUATION METHODS FOR NUCLEAR CLASS 1 PIPING WITH CLASS 2 OR 3 PIPING

E. C. Rodabaugh

Manuscript Completed – May 23, 1983
Date Published – June 1983

Report Prepared by
E. C. Rodabaugh Associates, Inc.
4625 Cemetery Road
Hilliard, Ohio 43026
under
Subcontract No. 19X-22252C

Work Performed for
U.S. Nuclear Regulatory Commission
Office of Nuclear Regulatory Research
under
DOE Interagency Agreement No. 40-550-75

NRC FIN No. B0474

OAK RIDGE NATIONAL LABORATORY
Oak Ridge, Tennessee 37830
operated by
UNION CARBIDE CORPORATION
for the
U.S. DEPARTMENT OF ENERGY
under Contract No. W-7405-eng-26

CONTENTS

	Page
NOMENCLATURE	v
ABSTRACT	1
1. INTRODUCTION	1
2. CODE 1 BASIS	4
3. CODE 2 BASIS	6
4. CORRELATIONS BETWEEN CODES 1 AND 2	12
4.1 Relationship Between i and C_2K_2	12
4.2 Comparison of Code 1 with Code 2 Basis, SA106 Grade B up to 400°F	13
4.3 Other Ferritic Materials and Temperatures	15
4.4 Austenitic Steels, Alloys 600 and 800	17
4.5 Temperature Effect, Piping Product Tests	19
4.6 Mean Stresses	19
5. HIGH-CYCLE FATIGUE	21
6. TEES	25
7. CODE 2 COVERAGE OF LOADINGS OTHER THAN MOMENTS	28
7.1 Allowance for Cyclic Pressure	28
7.2 Allowance for Thermal Gradients	29
7.3 Use of Eq. (2) for Combined Loadings	29
7.4 Code 2 Cumulative Usage Equation	30
7.5 Primary Stress Protection, High Temperatures	31
8. SUMMARY	32
8.1 Chapters 2–4, Fatigue Evaluation up to 10^6 Cycles	32
8.2 Chapter 5, High-Cycle Fatigue	32
8.3 Chapter 6, Tees	32
8.4 Chapter 7, Loadings Other than Moments	32
REFERENCES	33
APPENDIX A. BACKGROUND OF THE K_e FACTOR	35
APPENDIX B. BASIS OF CODE 1 FATIGUE DESIGN CURVES	43
APPENDIX C. COMPARISONS OF CARBON STEEL AND AUSTENITIC STAINLESS STEEL PIPING PRODUCT MOMENT FATIGUE TESTS	51

NOMENCLATURE

C_1	primary-plus-secondary stress indices for pressure
C_2	primary-plus-secondary stress indices for moment
C_3	primary-plus-secondary stress indices for thermal gradients
C_{2b}	primary-plus-secondary stress index, moment loading, tee branch
C_{2r}	primary-plus-secondary stress index, moment loading, tee run
D_o	pipe OD
E	modulus of elasticity
f	Code 2 cycle-dependent factor ranging from 1.0 for 7,000 cycles to 0.5 for 100,000 cycles or more
h	elbow parameter, tR/r^2
i	Code 2 stress intensification factor
K_1	peak stress indices for pressure
K_2	peak stress indices for moment
K_3	peak stress indices for thermal gradients
K_{2b}	peak stress index, moment loading, tee branch
K_{2r}	peak stress index, moment loading, tee run
K_e	elastic-plastic adjustment factor, see Eq. (3)
M	moment
M_i	range of resultant moment
M_c	range of resultant moment caused by thermal expansion
N	number of design cycles
N_f	number of cycles to failure
P_o	range of service pressure
P	internal pressure
r	mean radius of pipe, branch pipe for tees
R	mean radius of pipe, run pipe for tees, or bend radius for elbows
S_a	Code 1 fatigue design stress amplitude
S_c	Code 2 allowable stress at cold (100°F) temperature
S_d	design stress with factor of safety of 2 on S_f
S_e	endurance limit (fatigue strength at ~10^{11} cycles)
S_E	Code 2 calculated stress range
S_f	failure stress, correlated with N_f
S_h	Code 2 allowable stress at hot (maximum) temperature

Preceding page blank

S_m	Code 1 allowable stress intensity
S_n	calculated primary-plus-secondary stress range, see Eq. (1)
S_p	calculated peak stress range, see Eq. (2)
S_s	Code 2 sustained load stress, see Eq. (6)
S_u	ultimate tensile strength of material
S_y	yield strength of material
t	wall thickness of pipe, branch pipe for tees
T	wall thickness of pipe, run pipe for tees
U	fatigue usage factor
X	$(1 - n)/[n(m - 1)]$, see Eq. (19)
Z	section modulus of pipe
Z_b	section modulus of tee branch pipe
Z_r	section modulus of tee run pipe
α	coefficient of thermal expansion
ΔT_1	thermal gradients, see Code 1 for detailed definitions
ΔT_2	thermal gradients, see Code 1 for detailed definitions
T_a	thermal gradients, see Code 1 for detailed definitions
T_b	thermal gradients, see Code 1 for detailed definitions
ν	Poisson's ratio

COMPARISONS OF ASME CODE FATIGUE EVALUATION METHODS FOR NUCLEAR CLASS 1 PIPING WITH CLASS 2 OR 3 PIPING

E. C. Rodabaugh*

ABSTRACT

The fatigue evaluation procedure used in the *ASME Boiler and Pressure Vessel Code, Sect. III, Nuclear Power Plant Components*, for Class 1 piping is different from the procedure used for Class 2 or 3 piping. The basis for each procedure is described, and correlations between the two procedures are presented. Conditions under which either procedure or both may be unconservative are noted.

Potential changes in the Class 2 or 3 piping procedure to explicitly cover all loadings are discussed. However, the report is intended to be informative, and while the contents of the report may guide future Code changes, specific recommendations are not given herein.

1. INTRODUCTION

Fatigue-based criteria for the evaluation of piping were introduced into the Piping Code, then American Standards Association (ASA) B31.1,† in the 1955 edition. These criteria were based on moment fatigue tests on piping components by Markl,[2] Markl and George,[3] and Markl.[4] The criteria involve use of stress intensification factors (i-factors) and stress limits related to cold (S_c) and hot (S_h) allowable stresses, modified by a factor f, which depends upon the number of design cycles.

The American Society for Mechanical Engineers (ASME) *Boiler and Pressure Vessel Code, Sect. III, Nuclear Vessels*, was initiated in 1963. It covered Class A, B, and C vessels, now called Class 1, 2, and 3 vessels. This Code, for Class A vessels, used a fatigue evaluation method that is based on fatigue tests of polished bars. It uses design fatigue curves in which the allowable design stress S_a is plotted against the number of design cycles N. Stress indices were introduced in the 1963 Code for the particular case of nozzles with cyclic pressure loading.

In 1969, ANSI B31.7, *Nuclear Power Piping* was published. It covered Class 1, 2, and 3 piping. For Class 1 piping, B31.7 adopted a fatigue

*E. C. Rodabaugh Associates, Inc., Hilliard, Ohio.

†In 1955, B31.1 covered all industrial piping. Later, it was split into American National Standards Institute (ANSI) B31.1, *Power Piping*; ANSI B31.3, *Chemical Plant and Petroleum Refinery Piping*; ANSI B31.4, *Refrigeration Piping*; and ANSI B31.8, *Gas Transmission and Distribution Piping*.

analysis method analogous to that used in the Nuclear Vessel Code. The concept of "stress indices" was expanded to cover pressure, moment, and thermal gradient loads for commonly used piping components. For Class 2 and 3 piping, ANSI B31.7 continued to use the fatigue evaluation method originally introduced in ASA B31.1 in 1955.

In 1971, Sect. III of the ASME Code was expanded to include vessels, pumps, valves, and piping; the title was changed from *Nuclear Vessels* to *Nuclear Power Plant Components*. With respect to the fatigue evaluation methods for piping, Sect. III adopted, with one difference, the rules contained in ANSI B31.7-1969. The difference concerns the adjustment for stresses that exceed $3S_m$ (conceptually, exceed the shakedown limit). This adjustment, as will become apparent in this report, is highly significant in correlations between Class 1 and Class 2 or 3 piping fatigue evaluation methods. The method used in ANSI B31.7 is described in Appendix A, along with a background discussion of the equivalent K_e factor introduced in Sect. III-1971 and currently used.

The present (1982) status of fatigue evaluation methods used in Sect. III can be briefly summarized as follows:

Class components	*Fatigue evaluation basis*
Class 1 vessels, pumps, valves, and piping	Design fatigue curves derived from polished bar fatigue test data, with K_e adjustment
Class 2 and 3 vessels,* pumps, and valves	None
Class 2 and 3 piping	Piping component fatigue tests, using stress intensification factors, moment loading only

The objective of this report is to show how the fatigue evaluation method for Class 1 piping correlates with that for Class 2 or 3 piping. The methods for Class 2 and 3 piping are identical. For brevity, we will identify those methods as "Code 2"; those for Class 1 piping are identified as "Code 1."

Chapters 2 and 3 of this report describe the fatigue evaluation procedures for Code 1 and Code 2, respectively. Chapter 4 indicates the correlations between Codes 1 and 2. These correlations are necessarily limited to moment loadings, because Code 2 covers only moment loading.

Chapter 5 on high-cycle fatigue is treated separately, because it is not apparent that either Code 1 or Code 2 adequately covers the fatigue evaluation of accumulated cycles of 10^7 or more. Chapter 6 discusses a difference between Codes 1 and 2 that is applicable only to tees. Chapter 7 contains an exploratory discussion of the possibility of extending Code 2 fatigue evaluation to cover (or more explicitly cover) loadings other than moments.

---

*A fatigue evaluation may be required for vessels designed to the alternative rules of NC-3200 (equivalent to ASME Boiler and Pressure Vessel Code, Sect. VIII, Div. 2).

Chapter 8 summarizes the observations contained in Chaps. 2–7. The report is intended to be informative and may provide a basis for future Code changes. However, no recommendations for such changes are included herein.

In reading the subsequent sections of this report, the expert on fatigue evaluation methods will recognize that, in both Code 1 and 2 methods, many simplifying approximations are involved. For example, use of the linear cumulative damage hypothesis can be inaccurate for certain sequences of loading. However, in addition to and perhaps justifying the simplifying approximations, the operating history of the piping systems must be postulated. Because the operating history extends 20 to 40 years into the future, its postulated details are deemed to be the most uncertain aspect of the fatigue evaluation method. The fatigue evaluation methods are based on test data in an environment like dry air. Environmental effects, such as corrosion or stress-corrosion-cracking, are not covered or, at best, are only partially covered by factors of safety on the test data.

2. CODE 1 BASIS

The Code 1 fatigue evaluation method* involves the calculation of the primary-plus-secondary stress range S_n by the equation:

$$S_n = C_1 \frac{P_o D_o}{2t} + C_2 \frac{M_i}{Z} + C_3 E_{ab} |\alpha_a T_a - \alpha_b T_b| , \tag{1}$$

and the peak stress range by the equation:

$$S_p = K_1 C_1 \frac{P_o D_o}{2t} + K_2 C_2 \frac{M_i}{Z} + \frac{1}{2(1-\nu)} K_3 E\alpha|\Delta T_1|$$

$$+ K_3 C_3 E_{ab} |\alpha_a T_a - \alpha_b T_b| + \frac{1}{1-\nu} E\alpha|\Delta T_2| . \tag{2}$$

If $S_n \leq 3S_m$ (conceptually, $2S_y$, the shakedown limit), S_p is divided by 2 to convert from stress range to stress amplitude. The Code 1 design fatigue curves (Figs. I-9.1, I-9.2, or I-9.3, depending upon the material) are entered with $S_p/2$, and design cycles N are read from the curves. If the anticipated number of cumulative fatigue cycles in operation is less than N, then the piping product (e.g., girth butt weld, elbow) is deemed to be acceptable.

If $S_n > 3S_m$, the strain range corresponding to the elastic-based calculation of stress range may be too low. With primary-plus-secondary stresses that exceed $2S_y$, shakedown to elastic response may not occur and plastic strains, in addition to the calculated elastic strains, may occur during each cycle. To provide a simple way to deal with this condition, Code 1 (NB-3228.3) permits the use of a simplified elastic-plastic analysis that involves multiplying S_p by K_e, where K_e is given by

$$K_e = 1 + \frac{1-n}{n(m-1)} \left(\frac{S_n}{3S_m} - 1\right) ; \quad \text{for } 3S_m \leq S_n \leq 3mS_n , \tag{3}$$

$$K_e = 1/n \quad \text{for } S_n > 3mS_m .$$

---

*Code 1 permits the use of the more general rules given in NB-3200; this report is restricted to the rules given in NB-3650, "Analysis of Piping Products."

Values of m and n are

Material	m	n
Carbon steel	3.0	0.2
Low-alloy steel and martensitic stainless steel	2.0	0.2
Austenitic stainless steel, nickel-chrome-iron, and nickel-copper	1.7	0.3

Tagart has prepared a description[4] of the basis of Eq. (3), which is included herein as Appendix A.

Code 1 Figs. I-9.1, I-9.2, and I-9.3 are based on strain-controlled, zero mean strain, fatigue tests of polished bars. The design fatigue curves were derived from the failure curves by incorporating a factor of safety of 2 on stress or 20 on cycles, whichever is more conservative. (The 20 on cycles controls at low cycles, the 2 on stress controls at high cycles.) An adjustment for the effect of mean stress is included in Fig. I-9.1 for ultimate tensile strength (UTS) $\leq$ 80 ksi. Appendix B contains a detailed discussion of Figs. I-9.1 and I-9.2.

Code 1 uses the linear cumulative damage hypothesis as expressed by:

$$U = \sum_{i}^{j} \frac{n_i}{N_i} \leq 1.0 \ , \tag{4}$$

where

n_i = number of cycles with amplitude S_i,
N_i = allowable number of cycles from Code 1 Fig. I-9.0 for S_i.

Each type of stress cycle with amplitude S_i must be identified from the postulated operating history of the piping system. There are usually ten or more of such identifiable cycles, each occurring n_i times. The total number of types of cycles is j.

3. CODE 2 BASIS

The Code 2 fatigue evaluation method involves the calculation of the stress *range* S_E by the equation

$$S_E = iM_c/Z \ . \tag{5}$$

If S_E satisfies the equation

$$S_E \leq f[1.25(S_h + S_c) - S_s] \ , \tag{6}$$

and $S_s \leq S_h$, the piping component is deemed to be acceptable from a fatigue evaluation standpoint.

The Code 2 method is based on the results of moment-loading fatigue tests given by Markl,[1] Markl and George,[2] and Markl.[3] The test arrangement for various piping products is indicated in Fig. 1. Test assemblies were mounted in the fatigue test machine and subjected to a preliminary load-deflection calibration. The assemblies were filled with water to

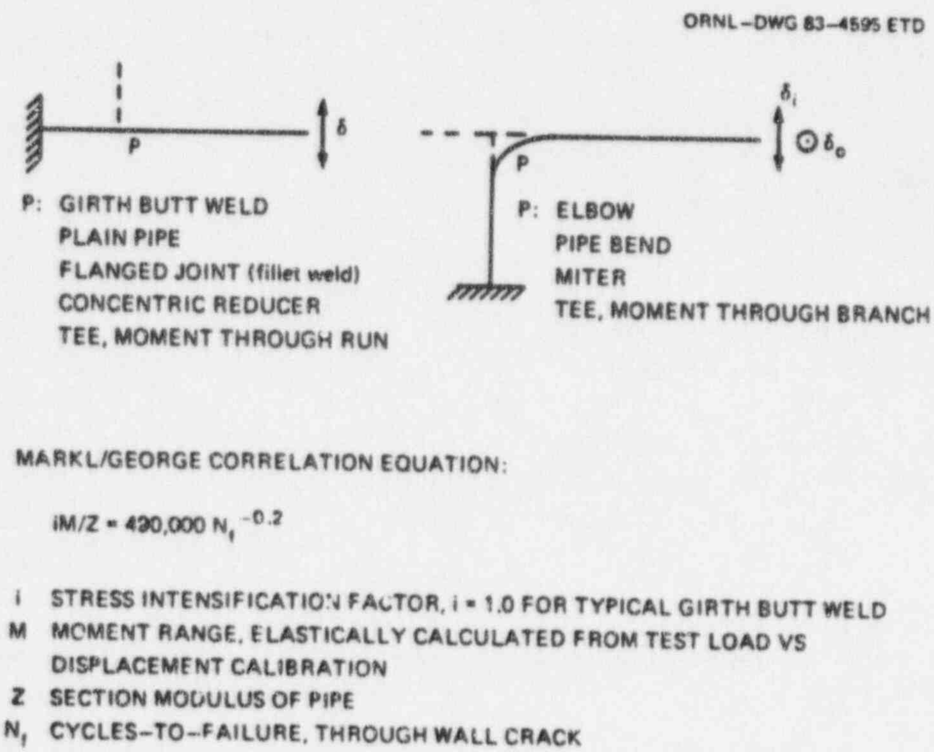

Fig. 1. Displacement-controlled, completely reversed cyclic moment tests on 4-in. nominal size, SA106 Grade B piping products at room temperature. *Source*: Refs. 1–3.

provide a ready means for detecting failure and were then flexed cyclically (completely reversed displacements) through a predetermined displacement until a leak that indicated a crack through the wall developed.

The results were reported as points on S_f vs N_f plots. N_f is the number of cycles to failure (crack through the wall). The corresponding nominal stress was computed by the ordinary beam formula, $S_f = WL/Z$. The load range W was taken from the load-deflection calibration, or for loads causing plastic deformation, from straight-line extrapolation of the elastic portion of the load-deflection calibration. The lever arm L was measured from the point of load application to the point of initial failure.

The test method is consistent with an elastic analysis of a piping system, even though calculated stresses may be above the material yield strength and some plastic deformation may occur. Accordingly, an adjustment analogous to the K_e used in Code 1 is not needed.

All tests were run on 4-in. nominal size piping components at room temperature. The material used to make the test specimens was American Society of Testing Materials (ASTM) A106 Grade B. The tensile strengths ranged from 62,400 to 86,300 psi; yield strengths ranged from 38,900 to 56,200 psi; and elongation for 2-in. gage section ranged from 32 to 55%. All welding was done manually using Fleetweld No. 5 electrodes. Most specimens were tested "as welded." A few girth butt weld specimens were stress relieved after welding and before testing with no detectable differences in the test results.

To make the test information useful to the piping designer, Markl developed a correlation of the form

$$iS_f = aN_f^{-b} , \tag{7}$$

where a and b are constants developed from the test data. Results of tests for girth butt welds are shown in Fig. 2, in which S_f and N_f are plotted on log scales. Equation (7) is shown in Fig. 2. It is a best fit of the test data with b = 0.2. The value of b = 0.2 was selected after evaluating test data for all types of piping products. Individual test series gave values of b ranging from 0.1 to 0.3, but most values were within 20% of 0.2, which represents a fair average. For girth butt welds, the best fit value of a is 490,000. Accordingly, Eq. (7) for a girth butt weld is

$$S_f = 490{,}000\ N_f^{-0.2}\ \text{(psi, range)} . \tag{8}$$

Markl's more general equation is

$$iS_f = 490{,}000\ N_f^{-0.2}\ \text{(psi, range)} , \tag{9}$$

where i = 1.0 for a girth butt weld and i is the fatigue-based stress intensification factor for piping products other than girth butt welds.

ORNL-DWG 83-4596 ETD

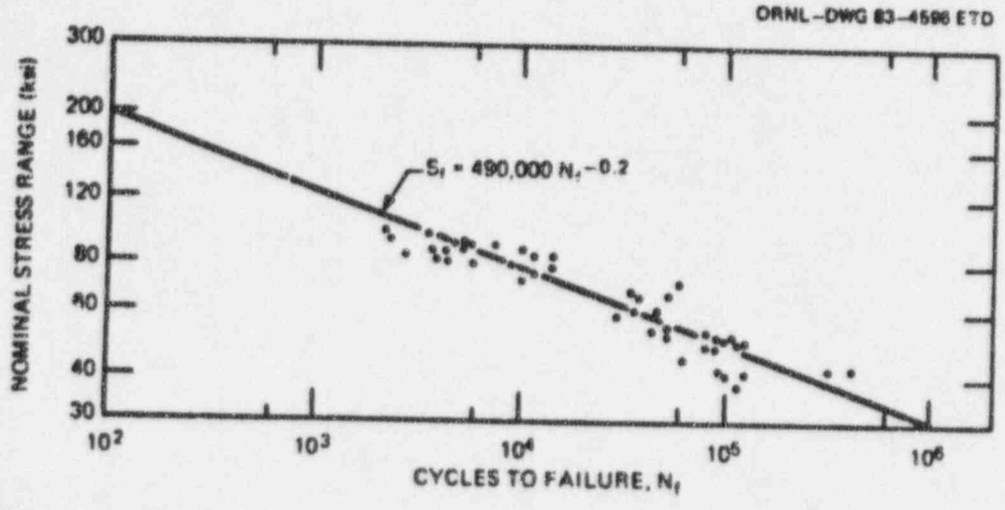

Fig. 2. Results of moment fatigue tests on girth butt welds. *Source*: Ref. 3.

Equation (9) does not appear in Code 2. The basis for the criteria contained in Code 2 was discussed by Markl.[4] His concept was that the calculated stress range S_E should be limited to

$$S_E \leq 1.6(S_c + S_h) \ , \tag{10}$$

where S_c is the allowable stress at the minimum temperature in the cycle and S_h is the allowable stress at the maximum temperature in the cycle. At that time (1955), the allowable stresses in the *Power Piping Code* were limited to $(5/8)S_y$, where S_y is the material yield strength at operating temperature. Accordingly, Eq. (10) is conceptually equivalent to

$$S_E \leq 2S_{ya} \ . \tag{11}$$

where S_{ya} is the average of the hot and cold yield strengths. Users of Code 1 will recognize that Eq. (11) is the equivalent of the shakedown criteria implied by $S_n \leq 3S_m$. However, the equivalence is not that straightforward, because S_E includes peak stresses, whereas S_n does not. Further, because the i's are referenced to the fatigue strength of a typical girth butt weld, S_E is not equal to either S_n or S_p (as discussed later, $i = C_2K_2/2$).

Equation (11) is an interesting step on the way to the Code 2 criteria, Eq. (6). However, the writers of the piping code in 1955 were faced with the broad problem of integrating room temperature test data on the fatigue life of A106 Grade B piping components into design guidance for many materials and temperatures. How to limit sustained (noncyclic) stresses, such as those caused by pressure and weight, was one aspect.

Applicability of the design guidance at elevated temperatures, where significant creep occurs, was a major concern. Eventually, after consideration of several proposed criteria, the criteria indicated by Eq. (6) were published in ASA B31.1-1955, *Code for Pressure Piping*.

Equations (6) and (9) are compared in Fig. 3. Noting that Eq. (9) is for *cycles to failure*, a factor of safety is needed for design guidance. Figure 3 includes a "design" line representing Eq. (9) with a factor of safety of 2 on stress, analogous to the factor of safety of 2 on stress used in Code 1. (The factor of 20 on cycles is also satisfied because $2^5 = 32$.) The design equation is then

$$iS_d = 245{,}000\ N^{-0.2}\ \text{(psi, range)}\ . \tag{12}$$

Assuming, as in Code 1, that fatigue at temperatures up to 650°F is not significantly different from that at room temperature, then Fig. 3 indicates that even for $S_s = 0$, Eq. (6) for A106 Grade B material at temperatures up to 650°F ($S_c = S_h = 15{,}000$ psi) has a factor of safety of 2 or greater up to ~400,000 cycles. The f-factor, which varies between 1 for 7,000 cycles to 0.5 for 100,000 or more cycles, gives the stepped variation between 7,000 and 100,000 cycles. The factor of safety is high at low cycles (e.g., 5.2 at 100 cycles). Comparisons between Eqs. (9) and (12) for materials other than SA106 Grade B are discussed in Sects. 4.3 and 4.4.

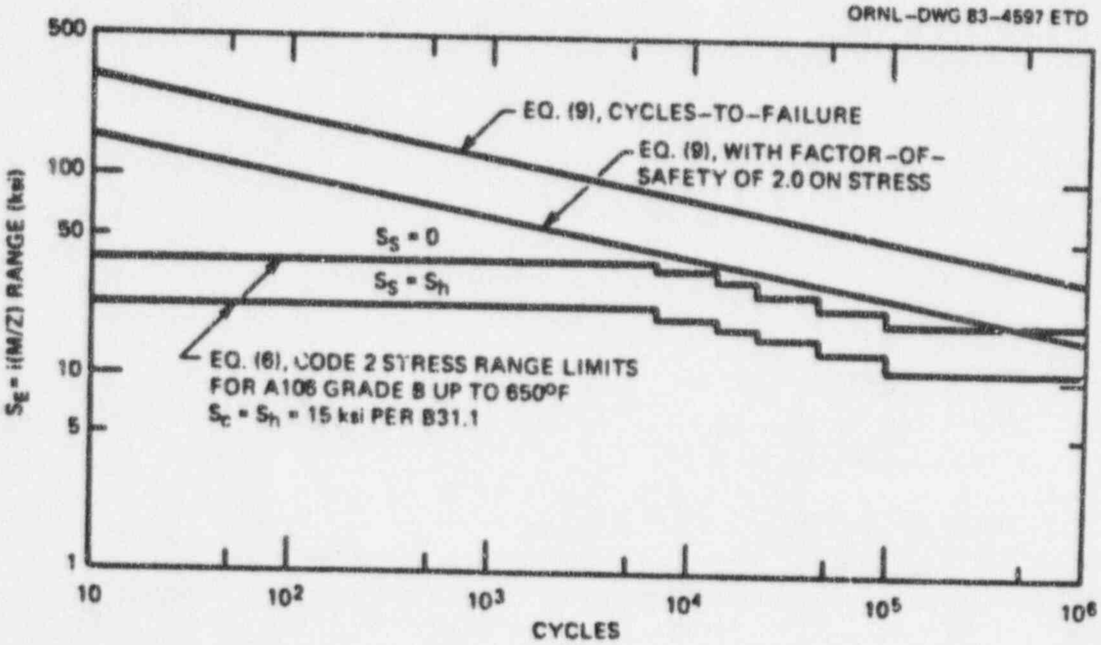

Fig. 3. Comparison of Eq. (9) with Code 2 allowable stresses for SA106 Grade B material.

Code 2, like Code 1, uses the linear cumulative damage hypothesis as expressed by the equation given in NC-3611.2(e)(3):

$$N = N_E + r_1^5(N_1) + r_2^5(N_2) + \ldots\ldots r_n^5(N_n) \; , \tag{13}$$

where

N_E = number of cycles at run temperature change ΔT_E for which the expansion stress S_E has been calculated;
$N_1, N_2, \ldots N_n$ = number of cycles for smaller temperature changes, $\Delta T_1, \Delta T_2, \ldots \Delta T_n$;
$r_1, r_2, \ldots r_n$ = $\Delta T_1/\Delta T_E, \Delta T_2/\Delta T_E \ldots \Delta T_n/\Delta T_E$.

The exponent of the r's, assuming S_E is proportional to ΔT_E, follows from the exponent of N in Eq. (9). Note that Eq. (13) does not include cyclic moments caused by other than restraint of free thermal expansion (e.g., cyclic moments caused by relief valve discharge). Equation (13) implies that there is no endurance limit (stress below which fatigue damage does not occur). This is deemed to be alright provided the N's are not greater than 10^6 cycles. Equation (13), of course, does not explicitly cover loadings such as pressure or thermal gradients (Sect. 7.4).

Equation (6) represents the fatigue evaluation introduced into the piping code in 1955. The right-hand side of Eq. (6) includes the calculated stress S_s that was defined as "... the sum of the longitudinal stresses due to pressure, weight and other sustained loads." An equation was given for calculating the longitudinal pressure stress: $S_{sp} = pd^2/(D^2 - d^2)$, where p = internal pressure, d = pipe ID, and D = pipe OD. This equation is reasonably correct for straight and curved pipe; it is not defined for reducing outlet tees. (Are the branch pipe or the run pipe dimensions to be used?) An appropriate method to be used in calculating the "longitudinal stresses due to weight and other sustained loads" was not given. Except for straight pipe, the longitudinal stress caused by a moment loading is *not* given by M/Z. Indeed, for elbows subjected to an in-plane bending moment, the maximum stress causing fatigue failure is in the hoop direction. To quantify how to calculate S_s, Code 2 now uses the criteria equation:

$$PD_o/4T + 0.75iM_A/Z + iM_C/Z \leq S_h + f(1.25S_c + 0.25S_h) \; , \tag{14}$$

where

P = design pressure,
M_A = resultant moment caused by weight and other sustained loads,
M_C = range of resultant moment caused by thermal expansion.

The intent was that $S_s = PD_o/4T + 0.75iM_A/Z$. With that equivalence, Eqs. (6) and (14) are the same for $f = 1.0$. In most applications, f is taken to be unity. The significance of S_s in a fatigue evaluation is discussed further in Sects. 4.6 and 4.7.

4. CORRELATIONS* BETWEEN CODES 1 AND 2

4.1 Relationship Between i and C_2K_2

Note under Eq. (9) that i is unity for a girth butt weld. The welds tested by Markl were typical of industrial practice for welds in carbon steel piping. The roots of the welds were not smooth, and the weld overlay on the outside surface was typically irregular and presumably included minor undercutting. Such welds are *not* the equivalent of polished bars that form the basis for Code 1 fatigue evaluation with the associated C_2 and K_2 moment-loading stress indexes. Accordingly, to compare Code 2 and Code 1 fatigue evaluations, a relationship between i and C_2K_2 must be established.

For elbows subjected to in-plane moment, the maximum principal stress σ_m is given by theory (for the elbow parameter h less than about one) as

$$\sigma_m = (1.8/h^{2/3})M/Z \ . \tag{15}$$

The validity of Eq. (15) has been confirmed by numerous tests in which strain gages were placed on elbows subjected to in-plane moment. The i-factor for elbows, with i = 1.0 for a typical girth butt weld, is

$$i = 0.9/h^{2/3} \ . \tag{16}$$

The fatigue tests[1] that led to Eq. (16) were in-plane moment tests. The fatigue failure locations and directions agreed very well with the theoretical location and direction of the maximum principal stress. However, i is exactly one-half of $1.8/h^{2/3} \cong C_2$. Because the failures occurred in the body of the elbows remote from welds, $K_2 = 1.0$ and

$$i = C_2K_2/2 \ . \tag{17}$$

Equation (17) is included in Code 2, NC-3673.2(b).

The elbow theory and fatigue tests provide the fundamental basis for Eq. (17). However, other evidence exists to confirm its general validity as discussed in the following.

If i = 1.0 for a typical girth butt weld and Eq. (17) is generally applicable, then we would expect that i = 0.5 for fatigue tests run on a straight pipe with polished surfaces, because $C_2 = K_2 = 1.0$. Such tests are not available, but Markl[1] included tests of "plain straight pipe." The resulting i-factor was 0.64. Fatigue tests of a plain straight pipe, with the fatigue machine used by Markl, poses a problem because almost

*Correlations are restricted to moment loadings, because Code 2 covers only moment loadings. See Chap. 7 for discussion of this aspect.

any feasible way of anchoring the pipe to the test frame will introduce a stress concentration. Markl solved the problem by using a tapered-wall forging, with about a 1:10 taper going from 0.237-in. nominal wall to ~0.6-in. nominal wall anchored-end. The surface of the test section was left "as-forged" to simulate a typical carbon steel pipe surface. Others,[6,7] using resonant bending testing in which the pipe is vibrated in the "free-free" mode with the pipe supported at the node points, also obtained i-factors for carbon steel pipe of about 0.65. Reference 7 also tested type 304 austenitic steel pipe and obtained an i-factor of 0.55, perhaps because of the better surface finish of austenitic steel pipe.

Moment fatigue tests[7-9] on girth butt welds with fusion root pass and/or the weld overlay ground flush also gave i-factors less than one.

References 10–15 give results of tests on branch connections or tees in which stresses caused by branch moment loads were measured with strain gages, after which the branch connections or tees were subjected to branch-loading cyclic moment fatigue tests. These tests also indicate that $i \cong C_2K_2/2$ (more specifically, $i \cong C_{2b}K_{2b}/2$).

4.2 Comparison of Code 1 with Code 2 Basis, SA106 Grade B up to 400°F

Having the relationship $i = C_2K_2/2$ and K_e as defined by Eq. (3), comparisons can be made between Code 1 and Eq. (12). The Code 1 S_a vs N curves can be adjusted for the K_e factor as described in the following paragraph. We start with the equation

$$K_eS_p = 2S_a \text{ (ranges)} , \tag{18}$$

where S_a is obtained from Code 1 Figs. I-9.1, I-9.2, or I-9.3 for the given number of cycles N. For example, for N (design cycles) = 10, S_a = 580 ksi for carbon steels with UTS $\leq$ 80 ksi. Because $S_p = K_2S_n$ and with K_e defined by Eq. (3), Eq. (18) becomes:

$$[1 + X(S_n/3S_m - 1)]K_2S_n = 2S_a \; ; \quad \text{for } 3S_m \leq S_n \leq 3_mS_m , \tag{19}$$

where $X = (1 - n)/[n(m - 1)]$. Solving Eq. (19) for S_n gives

$$S_n = \{(X - 1)K_2 + [(X - 1)^2K_2^2 + 8XK_2S_a/3S_m]^{1/2}\}/(2XK_2/3S_m) . \tag{20}$$

Also,

$$S_n = 2nS_e/K_2; \quad \text{for } S_n > 3mS_m , \tag{21}$$

and

$$S_n = 2S_a/K_s; \quad \text{for } S_n < 3S_m . \tag{22}$$

After determining S_n by Eq. (20), the peak stress is

$$S_p = K_s S_n . \tag{23}$$

Figure 4 shows the Code 1 S_a vs N curve, Code Fig. I-9.1, for UTS $\leq$ 80 ksi. Also shown, as dashed lines, are the adjusted (for K_e) curves for a carbon steel with S_m = 20 ksi, m = 3, n = 0.2, X = 2.0, such as SA106 Grade B at temperatures up to 400°F. An example of the development of the dashed curves, for N = 10^3 K_s = 2.0, is:

1. At N = 10^3, S_a = 83 ksi (from Code Table I-9.1).
2. Equation (20) with X = 2.0, K_s = 2.0, and $3S_m$ = 60 ksi gives S_n = $[2 + (4 + 32 \times 83/60)^{1/2}]/(8/60)$ = 67.1 ksi.
3. Because $S_n > 3S_m$, Eq. (20) applies; not Eq. (21) or (22).
4. Equation (23): $S_p = 2 \times 67.1 = 134$ ksi.
5. S_p is plotted at N = 10^3 to establish a point on the dashed line labeled K_s = 2.

This procedure is repeated to obtain other points on the dashed lines in Fig. 4. The K_e adjustment stops to the right when $S_n = 3S_m$ and there is a portion of the dashed curves at the extreme left where Eq. (21) controls.

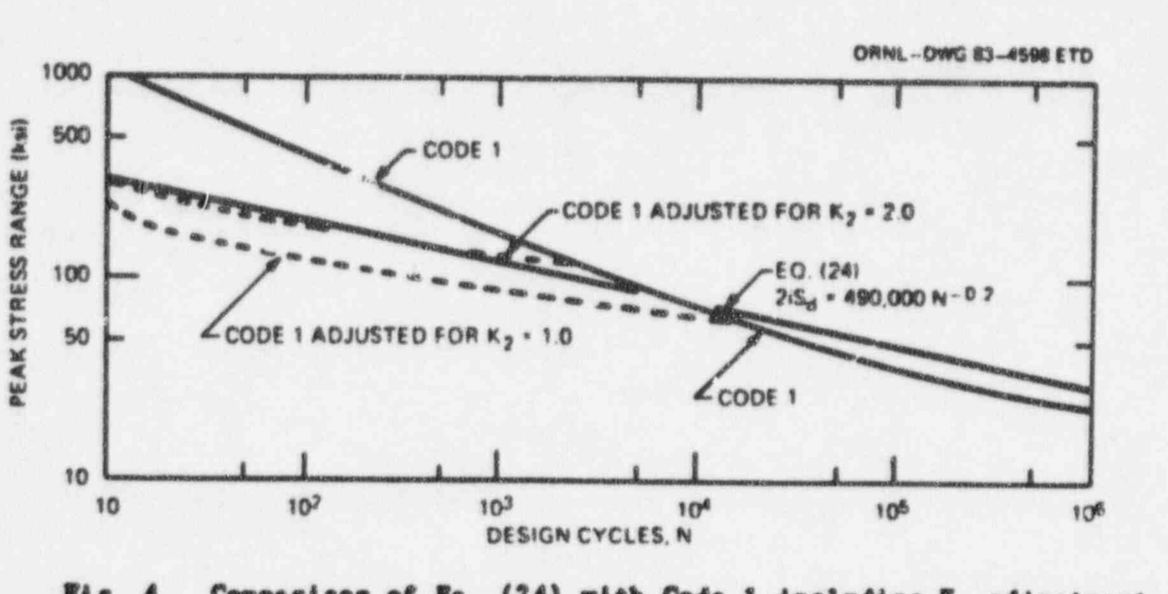

Fig. 4. Comparison of Eq. (24) with Code 1 including K_e adjustment, SA106 Grade B up to 400°F.

Equation (12), for Code 2, is a design cycles equation with a factor of safety of 2 on stress. However, because of the relationship of Eq. (17), $i = C_2K_2/2$, the appropriate comparison is between $2iS_d$ and $S_p = K_2S_n$:

$$2iS_d = 490{,}000\ N^{-0.2}\ \text{(psi, range)}\ . \tag{24}$$

Figure 4 includes Eq. (24). It is apparent in Fig. 4 that agreement between $2iS_d$ and S_p for $K_2 = 2$ is good up to ~20,000 cycles. $K_2 = 2$ is approximately that used for a girth butt weld. For $K_2 = 1$, Code 1 is more conservative than Eq. (24). $K_2 = 1$ is used for elbows; direct comparison of elbow fatigue tests with Code 1 fatigue evaluation also indicates that Code 1 is conservative as applied to carbon steel elbows.[16,17]

The high-cycle end of Fig. 4 will be discussed in Chap. 5.

4.3 Other Ferritic Materials and Temperatures

Figure 4 constitutes the most significant correlation between Codes 2 and 1, because Markl's fatigue tests were run on piping components made of SA106 Grade B carbon steel at room temperature and because Code 1 design fatigue curves in Fig. I-9.1 for UTS $\leq$ 80 ksi, as discussed in Appendix B, are based on tests at room temperature of materials like SA106 Grade B.

Table 1 shows correlations between Codes 2 and 1 in the form of ratios of design fatigue stresses to Eq. (24). For Code 2, Eq. (24) is multiplied by $(S_c + S_h)_{mt}/(S_c + S_h)_r$, where the subscript "mt" indicates the values of S_c and S_h for the indicated material and temperature; subscript "r" indicates the reference SA106 Grade B at 100°F ($S_c = S_h = 15$ ksi).

Code 1 basic design fatigue curves group materials (e.g., SA106 Grades A, B, and C) do not depend on temperature.* However, the design fatigue stresses are material and temperature dependent when the K_e factor is involved, because K_e is a function of S_m, which is material and temperature dependent.

Table 1 ratios are numerical analogs of eight graphs like Fig. 4. We previously noted that Fig. 4 showed that the agreement between Eq. (24) and S_p for $K_2 = 2.0$ for A106 Grade B carbon steel was good up to ~20,000 cycles. In Table 1 the ratios are shown: 0.96, 0.97, 1.09, and 0.98 for $N = 10$, 10^2, 10^3, and 10^4, respectively.

Code 2 ratios are independent of cycles N whereas the Code 1 ratios depend upon N. For small N, K_e may be equal to $1/n$, in which case the ratios are independent of S_m and thus independent of the material (within the group) and temperature. For large N, $K_e = 1.0$, in which case the ratios are also independent of S_m and thus independent of the material (within the group) and temperature. Within the range between $K_e = 1/n$ and

---

*Provided E used in calculating the stresses is the same as those shown in Code 1 Fig. I-9.0.

Table 1. Ratios[a] of design fatigue stresses to Eq. (24) for ferritic materials

N^b (S)	Basis[c]	Temperature 100°F				Temperature 700°F			
		SA106A	SA106B	SA106C	SA672-J100	SA106A	SA106B	SA106C	SA672-J100
10 (309)	Code 2	0.80	1.00	1.17	1.67	0.79	0.98	1.14	1.67
	Code 1, $K_s = 1$	0.75^d	0.75^d	0.75^d	0.64	0.75^d	0.75^d	0.75^d	0.64
	Code 1, $K_s = 2$	0.85	0.96	1.04	1.00	0.80	0.87	0.93	1.00
10^2 (195)	Code 2	0.80	1.00	1.17	1.67	0.79	0.98	1.14	1.67
	Code 1, $K_s = 1$	0.57	0.65	0.71	0.72	0.54	0.59	0.64	0.72
	Code 1, $K_s = 2$	0.85	0.97	1.07	1.19	0.80	0.88	0.95	1.19
10^3 (123)	Code 2	0.80	1.00	1.17	1.67	0.79	0.98	1.14	1.67
	Code 1, $K_s = 1$	0.62	0.71	0.78	0.90	0.58	0.64	0.69	0.90
	Code 1, $K_s = 2$	0.95	1.09	1.20	1.30^e	0.89	0.98	1.06	1.30^e
10^4 (77.7)	Code 2	0.80	1.00	1.17	1.67	0.79	0.98	1.14	1.67
	Code 1, $K_s = 1$	0.73	0.84	0.93	1.07^e	0.68	0.75	0.82	1.07^e
	Code 1, $K_s = 2$	0.98^e	0.98^e	0.98^e	1.07^e	0.98^e	0.98^e	0.98^e	1.07^e
10^5 (49.0)	Code 2	0.80	1.00	1.17	1.67	0.79	0.98	1.14	1.67
	Code 1, $K_s = 1$	0.82^e	0.82^e	0.82^e	0.96^e	0.82^e	0.82^c	0.82^e	0.96^c
	Code 1, $K_s = 2$	0.82^e	0.82^e	0.82^e	0.96^e	0.82^e	0.82^e	0.82^e	0.96^e
10^6 (30.9)	Code 2	0.80	1.00	1.17	1.67	0.79	0.98	1.14	1.67
	Code 1, $K_s = 1$	0.81^e	0.81^e	0.81^e	1.09^e	0.81^e	0.81^e	0.81^e	1.09^e
	Code 1, $K_s = 2$	0.81^e	0.81^e	0.81^e	1.09^e	0.81^e	0.81^e	0.81^e	1.09^e

[a] Ratios to $S = 21S_d = 490{,}000\ N^{-0.2}$, Eq. (24).

[b] $S = 490\ N^{-0.2}$, ksi.

[c] Code 2, Eq. (24) x $(S_c + S_h)_{mt}/(S_c + S_h)_r$, see text.
Code 1, S_p by Eq. (23).

[d] Indicates that $S_n > 3mS_m$, $K_e = 1/n$, and $S_p = 2mS_a$. S_a = fatigue design stress from Code 1 Table I-9.1 for listed N, interpolated for SA672-J100.

[e] Indicates that $S_n < 3S_m$, $K_e = 1.0$, and $S_p = 2S_a$.

$K_e = 1.0$, Codes 2 and 1 give similar changes in design fatigue stresses as a function of material and temperature.

SA672-J100 is a low-alloy steel, welded pipe material. It is seldom used in nuclear power plant piping but was included to illustrate a potential hazard in the Code 2 fatigue evaluation procedure. SA672-J100 has a specified minimum S_u of 100 ksi, S_y of 83 ksi, $S_c = S_h = 25$ ksi, and $S_m = 33.3$ ksi. Being listed as a low-alloy steel, $m = 2$, $n = 0.2$, and $X = 4$ as contrasted to SA106 Grades A, B, and C for which $m = 3$, $n = 0.2$, and $X = 2$. Values of S_a were obtained from Code Table I-9.1 by linear interpolation between values given for UTS $\leq$ 80 and UTS = 115–130 (S_u of 80 and 115 were used in the interpolation).

It can be seen in Table 1 that Code 2 permits a fatigue design stress for SA672-J100 that is 1.67 times that given by Eq. (24) for SA106 Grade B at 100°F. In contrast, Code 1, for $K_s = 2.0$ (e.g., a girth butt weld), permits a fatigue design stress that is, for most N, about equal to that for SA106 Grade B at 100°F. Unfortunately, no tests are available on girth butt welds in SA672-J100 pipe. As mentioned previously, Markl's tests were run on piping components made of materials with S_u ranging from 62.4 to 86.3 ksi, and S_y ranging from 38.9 to 56.2 ksi. However, fatigue failures in girth butt welds may be related to the properties of the weld metal or heat-affected zone rather than the base metal. We would speculate that girth butt welds in SA672-J100 pipe would not be much better than girth butt welds in SA106 Grade B, and in this particular respect, Code 1 is probably more accurate than Code 2. Note, however, that ratios in Table 1 are to the basic piping product fatigue curve, Eq.(24), and that Code 2 allowable fatigue design stresses, as illustrated in Fig. 3, contain a large margin for a low number of cycles.

A somewhat analogous situation exists in ANSI B31.3-1980, *Chemical Plant and Petroleum Refinery Piping*, where changing the allowable stress basis from a factor of 1/4 to 1/3 on S_u increased allowable design fatigue stresses by a factor of 4/3 for some materials and temperatures (e.g., for A106 Grade B from 15 to 20 ksi for temperatures up to 400°F).

4.4 Austenitic Steels, Alloys 600 and 800

Available fatigue test data on piping components made of type 304 austenitic stainless steel and dimensional equivalent piping components made of SA106 Grade B carbon steel are abstracted in Appendix C. These data indicate that SA106 Grade B components are slightly stronger than type 304 components. Accordingly, it is pertinent to continue comparisons with Eq. (24).

Figure 5 shows comparisons between Eq. (24), $2iS_d = 490{,}000\ N^{-0.2}$, and Eq. (23), $S_p = K_s S_m$. Figure 5 is for an austenitic steel with S_m = 20 ksi (e.g., SA312 type 304 at 100°F). For austenitic steels (and alloys 600 and 800), m = 1.7, n = 0.3, and X = 3.333.

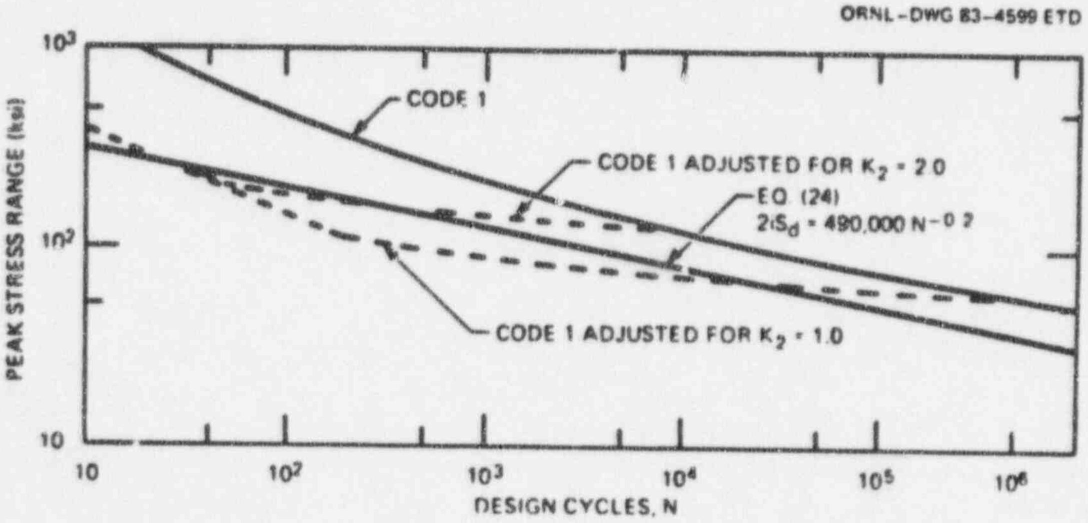

Fig. 5. Comparison of Eq. (24) with Code 1 including K_e adjustment, SA312 type 304 at 100°F.

Figure 5 indicates that fair agreement exists between Eq. (24) and S_p for $K_s = 2.0$ up to 10^3 cycles. However, for $N > 10^4$, Code 1 allowable stresses are 1.5 to 1.7 times those given by Eq. (24). If, as suggested by the data in Appendix C, Eq. (24) is about right or slightly unconservative for 304 material at 100°F, then Code 1 is unconservative. A similar relationship is apparent for $K_s = 1.0$ for N greater than ~10^5 cycles.

Table 2, like Table 1, shows correlations between Code 2 and Code 1 in the form of ratios of design fatigue stresses to Eq. (24). We previously noted that Fig. 5 showed agreement between Eq. (24) and S_p for 304 at 100°F and $K_s = 2.0$ up to 10^3 cycles. In Table 2 the ratios are shown: 1.26, 0.92, and 1.14 for N = 10, 10^2, and 10^3 cycles, respectively.

It is apparent in Table 2 that Code 2 also assigns higher allowable fatigue design stresses to 304 than to SA106 Grade B, by a factor of 1.25. This is contradictory to the test data on piping products shown in Appendix C.

Table 2. Ratios[a] of design fatigue stresses to Eq. (24) for 304 austenitic stainless steels and alloys 600 and 800

N[b] (S)	Basis[c]	Temperature 100°F				Temperature 800°F			
		304	304L	Alloy 600	Alloy 800	304	304L	Alloy 600	Alloy 800
10 (309)	Code 2	1.25	1.05	1.33	1.25	1.13	0.96	1.18	1.24
	Code 1, $K_s = 1$	1.26[d]	1.26[d]	1.26[d]	1.26[d]	1.26[d]	1.26[d]	1.26[d]	1.26[d]
	Code 1, $K_s = 2$	1.26[d]	1.26[d]	1.26[d]	1.26[d]	1.26[d]	1.26[d]	1.26[d]	1.26[d]
10^2 (195)	Code 2	1.25	1.05	1.33	1.25	1.13	0.96	1.18	1.24
	Code 1, $K_s = 1$	0.74[d]	0.74[d]	0.74[d]	0.74[d]	0.74[d]	0.74[d]	0.74[d]	0.74[d]
	Code 1, $K_s = 2$	0.92	0.82	0.92	0.92	0.77	0.74[d]	0.92	[illegible]
10^3 (123)	Code 2	1.25	1.05	1.33	1.25	1.13	0.96	1.18	1.24
	Code 1, $K_s = 1$	0.71	0.63	0.71	0.71	0.59	0.54	0.71	0.71
	Code 1, $K_s = 2$	1.14	1.00	1.14	1.14	0.94	0.84	1.14	1.14
10^4 (77.7)	Code 2	1.25	1.05	1.33	1.25	1.13	0.96	1.18	1.24
	Code 1, $K_s = 1$	0.92	0.81	0.92	0.92	0.76	0.69	0.92	0.92
	Code 1, $K_s = 2$	1.52[e]	1.34	1.52[e]	1.52[e]	1.25	1.11	1.52[e]	1.52[e]
10^5 (49.0)	Code 2	1.25	1.05	1.33	1.25	1.13	0.96	1.18	1.24
	Code 1, $K_s = 1$	1.29	1.13	1.29	1.29	1.06	0.94	1.29	1.29
	Code 1, $K_s = 2$	1.53[e]	1.53[e]	1.53[e]	1.53[e]	1.53[e]	1.53[e]	1.53[e]	1.53[e]
10^6 (30.9)	Code 2	1.25	1.05	1.33	1.25	1.13	0.96	1.18	1.24
	Code 1, $K_s = 1$	1.68[e]	1.64	1.68[e]	1.68[e]	1.52	1.35	1.68[e]	1.68[e]
	Code 1, $K_s = 2$	1.68[e]	1.68[e]	1.68[e]	1.68[e]	1.68[e]	1.68[e]	1.68[e]	1.68[e]

[a]Ratios to $S = 21S_d = 490{,}000\ N^{-0.2}$, Eq. (24).

[b]$S = 490\ N^{-0.2}$, ksi.

[c]Code 2, Eq. (24) x $(S_c + S_h)_{mt}/(S_c + S_h)_r$, see text.
Code 1, S_p by Eq. (23).

[d]Indicates that $S_n > 3mS_m$, $K_e = 1/n$, and $S_p = 2nS_a$. S_a ~ fatigue design stress from Code 1 Table I-9.1 for listed N.

[e]Indicates that $S_n < 3S_m$, $K_e = 1.0$, and $S_p = 2S_a$.

4.5 Temperature Effect, Piping Product Tests

As discussed in Appendix B, Code 1 design fatigue curves are dependent on temperature through the dependence on modulus of elasticity E. Code 1, NB-3222.4(e)(4), indicates that the calculated value of stress amplitude should be multiplied by E/E', where E' is the modulus used in the calculation and E is the modulus given on the design fatigue curve. In Class 1 piping (NB-3672.5), the piping system analyses are based on the hot modulus E_h, but calculations of expansion stresses are multiplied by E_c/E_h, where E_c is the cold modulus. To the extent that E given on the design fatigue curves is E_c, NB-3222.4(e)(4) and NB-3672.5 agree with each other. However, this is not quite the case at present (1982), for example, for 304 stainless steel at 70°F, E = 28.3 x 10^6 psi, whereas the value of E shown on the design fatigue curve is 26.0 x 10^6 psi.

References 18–20 include a few fatigue tests of girth butt welds and elbows at room temperature and at 550°F. There is no apparent effect of a temperature of 550°F with respect to room temperature tests. The ratios of room temperature modulus to the 550°F modulus are about 1.1 for both SA106 Grade B and type 304 stainless steel.

4.6 Mean Stresses

As discussed in Appendix B, Code 1 design fatigue curves include an adjustment for the maximum effect of mean stress. The S_s term in Eq. (6) might also be considered as a mean stress adjustment. However, if so considered, it would apply for all cycle stress levels and would be more severe than Code 1. For example, as indicated in Fig. 3, if $S_s = S_h$ (the maximum permissible value of S_s), the allowable design fatigue stresses are reduced to 60% of those permitted with $S_s = 0$.

In piping systems, each time there is a start-up and shutdown, which produces the (usually) major cycle of expansion stress range, the pressure also cycles from zero to the operating pressure and back to zero and there is also a cycle of thermal gradients. Noting that S_s includes weight loading, and that at each start-up and shutdown cycle, the contained fluid weight might change significantly, that portion of S_s might also "cycle." Accordingly, S_s might be viewed as a crude allowance for cyclic loads other than cyclic moments. The role of S_s in a fatigue evaluation is discussed further in Chap. 7.

Most fatigue test data on piping products have been run on specimens with the welds "as-welded" and, hence, had high mean stresses from residual weld stresses. To the extent that failures occurred at welds (girth butt welds, girth fillet welds, and welds in fabricated tees), these tests (even though completely reversed displacement or load) may have included some effect of mean stress.

Some moment piping product fatigue tests have been run with a constant pressure inside the test specimen.[13,14,18–22] In these tests, internal pressures were approximately equal to the maximum design pressure. The constant pressure produces a mean stress, although the maximum stress caused by pressure was usually significantly less than that caused by the moment range, and the maximum pressure-stress location and direction does not coincide with the maximum moment-stress location and direction. Accordingly, the effect of mean stress caused by internal pressure would be expected to be small, and indeed, the test data indicate no significant difference between tests with and without internal pressure.

Reference 22 also includes tests on carbon steel branch connections in which simulated misalignment stresses of M/Z = 10, 15, 20, or 25 ksi were imposed along with cyclic stress amplitudes of 3 to [illegible] ksi. These were high-cycle fatigue tests (N_f between 5×10^6 and 10^7), and mean stresses were high compared with cyclic stresses. Nevertheless, there was no significant difference between results with the lowest and highest mean stress.

In summary, available test data on piping products do not indicate that mean stresses are significant. In all cases the stress range was the significant aspect in the piping product test fatigue failures.

5. HIGH-CYCLE FATIGUE

A significant number of fatigue failures (leaks) have occurred in small-sized nuclear power plant piping. These have been related to vibration of the piping where the number of accumulated cycles can be very large in a relatively short period of calendar time. For example, at a vibration frequency of 100 Hz, 3.2×10^9 cycles accumulate in 1 year. Large numbers of accumulated cycles can be caused by turbulent mixing of hot and cold fluids or by flow-induced structural vibration (e.g., in steam generator tubes).

The conditions leading to high accumulated cycles are difficult to anticipate and have not been included in routine evaluations of nuclear power plant piping. However, if vibration is observed in preoperational testing or in service, appropriate design fatigue stress limits are needed to assess the significance of such vibrations.

Code 1 design curves provide values for allowable stress amplitude S_a for up to 10^6 cycles. NB-3222.4 and NB-3653.5 contain implications that S_a at 10^6 cycles is a design endurance limit. Furthermore, the footnote to NB-3222.5 says, "The endurance limit shall be taken as two times the S_a value at 10^6 cycles in the applicable fatigue curve of Fig. I-9.0." The factor of 2 here removes the safety factor in Fig. I-9.0.

Using S_a at 10^6 cycles as an endurance limit leads to a usage factor U of zero for any stress amplitude less than S_a at 10^6, regardless of the number of cycles. For example, if S_p were calculated to be 50,000 psi in a 304 stainless steel piping component, then U = 0 even for 10^9 cycles. As discussed in Appendix B, a more defensible value of allowable design stress amplitude S_a for 304 material at 10^9 cycles (Curve C) is 13,900 psi. By using S_a at 10^6 cycles = 26,000 psi as an endurance limit, the factor of safety of 2 on stress might be fully used up and failure (leak) would be about a 50% probability for this example with S_p = 50,000 psi, N = 10^9 cycles, 304 material.

Code 2 allowable design stresses for $N > 10^6$ are given by Eq. (6) with f = 0.5. Comparisons between Codes 1 and 2 (range basis) are shown in Table 3. The last column of Table 3 shows our estimate of an appropriate value of the endurance limit S_e for an effectively infinite number of cycles ($N = 10^{11}$), where S_e is adjusted for the maximum effect of mean stress and contains a factor of safety of 2 on stress. For type 304 stainless steels, the estimate comes from Appendix B.* Our estimate of S_e for ferritic steels is discussed in the following paragraphs.

Equation (9) is based on Markl's test data that covered a range of cycles from 10 to 10^6. Markl noted that his data on piping products, other than plain straight pipe, gave no evidence at all of trending to an asymptotic value (endurance limit) within the range of cycles covered. Fatigue test results on branch connections in Ref. 22 indicate that Eq. (9) is valid up to 10^7 cycles, with some indication of an endurance limit

---

*The estimated value is the value at 10^{11} cycles on the proposed Curve C.

Table 3. Comparisons of allowable design stress ranges at high cycles and estimate of endurance limit S_e

Material	Temperature (°F)	Allowable design stress range (ksi)			Endurance range estimate, S_e (ksi)
		Code 1[a]	Code 2[b]		
			$S_s = 0$	$S_s = S_h$	
SA106 Grade B	≤650	25.0	37.5	22.5	14
SA106 Grade A	≤650	25.0	30.0	18.0	14
SA106 Grade C	≤650	25.0	43.8	26.2	14
SA672-J100	≤650	40.0	62.5	37.5	14?
SA312 type 304	100	52.0	47.0	28.2	27
	800	52.0	42.5	27.3	27
SA312 type 304L	100	50.5[c]	39.2	23.6	27
	800	41.8[c]	35.9	22.9	27

[a]Values of $2S_a$ at 10^6 cycles. The factor of 2 converts amplitude to range.

[b]Values of $2S_E$ by Eq. (6). The factor of 2 incorporates the relationship $2i = C_2K_2$ and the Code 2 f-factor for N > 100,000 is 0.5, hence $2S_E = 1.25\ (S_c + S_h) - S_s$.

[c]K_e adjustment is applicable.

around 10^8 cycles. At 10^8 cycles, Eq. (9) gives $iS_f = 12.3$ ksi. Dividing this by 2, to obtain a factor of safety of 2 on stress, and multiplying by 2, to account for $2i = C_2K_2$, leads to an estimate of S_e (range) of 12.3 ksi.

High-cycle fatigue for austenitic steels is discussed in Appendix B. One of the proposed curves (Curve A) is simply an extrapolation of the present Code 1 using the equation (for $E = 28.3 \times 10^6$ psi):

$$S_a = 9159/\sqrt{N} + 47.35 \ . \tag{25}$$

In this extrapolation, adjustment for mean stress was not considered necessary, because S_a was presumed to be greater than the yield strength of the material.

If we similarly extrapolate the present Code 1 curve of Fig. I-9.1 for UTS ≤ 80 ksi and apply the adjustment for maximum effect of mean stress (see Appendix B, Table B.1), then we obtain $S_a = 7.43$ ksi at 10^{11}

cycles. This leads to an estimate of S_e (range) of 2 x 7.43 = 14.8 ksi vs 12.8 ksi by Eq. (9) at 10^8 cycles.

Some additional guidance can be obtained from fatigue tests of butt-welded joints in plates. Reference 23 contains a compilation of such data. In particular, Fig. B6 of Ref. 23 covers butt welds (reinforcement left on) in structural carbon steels, with failure points out to 2 x 10^6 cycles. The data, like Markl's, show no evidence of an endurance limit. Expressed in the form $S_f = aN_f^{\,b}$, the best-fit constants a and b give

$$S_f = 920\ N_f^{-0.276}\ \text{ksi}\ . \tag{26}$$

Reference 23 data cover from 10^4 to 2 x 10^6 cycles; whereas Markl's data cover from 2 x 10^3 to 4 x 10^8 cycles. In the region of overlap, Eqs. (9) and (26) agree fairly well with each other even though a butt weld in plate is not the same as a girth butt weld in pipe. Reference 23 data are heavily weighted by results between N_f = 5 x 10^5 and N_f = 2 x 10^6. For $N_f = 10^7$, it gives S_f = 10.8 ksi, which corresponds to S_e = 10.8 ksi, after dividing by 2 for the factor of safety and multiplying by 2 for $2i = C_2K_2$.

Reference 24 gives data on fatigue properties for butt-welded joints in SM50 B high tensile structural steel plates (S_u = 82.7 ksi and S_y = 71 ksi). These data cover the range from $N_f = 10^4$ to $N_f = 10^7$, with a few "runout" points at 2 x 10^7 cycles. These tests also give lower stresses than Eq. (9) at 10^7 cycles [~14.5 ksi vs the Eq. (9) value of 19.5 ksi]. Reference 24 data suggest a value for S_e of ~14.5 ksi.

References 23 and 24 tests were run in reversed tension; hence, they include a mean stress effect. Markl's tests were reversed bending. Possibly this mean stress effect is a major reason for lower fatigue failure stress ranges at high cycles in Refs. 23 and 24 than obtained from Eq. (9).

SA672-J100 is a high-strength, low-alloy ferritic steel with specified minimum S_u = 100 ksi and S_y = 83 ksi. Reference 25, in particular Fig. 5 therein, indicates the variation in S_f at 2 x 10^6 cycles with UTS for butt welds (reinforcement left on) in ferritic steel plates. The data cover a range of S_u from 55 to 150 ksi. There is, on the average, an increase in S_f with S_u of ~60% between S_u of 55 and 100 ksi and possibly a decrease in S_f with further increases in S_u. However, the scatter of the data at S_u = 100 ksi is such that it might be imprudent to depend upon any increase in S_f with S_u. Reference 25 data indicate that, for 0 to tension loading, 2 x 10^6 cycles, S_f is not less than 17 ksi for all UTS values covered. When divided by 2, for a factor of safety, and multiplied by 2 for $2i = C_2K_2$, the value of $2S_d$ at 2 x 10^6 cycles is 17 ksi. Our estimate that S_e = 14 ksi, in relation to Ref. 25 data, implies a reduction in fatigue strength by a factor of 14/17 = 0.82 between 2 x 10^6 and 10^{11} cycles. In view of Ref. 25 data, we have shown S_e for SA672-J100 in Table 3 as 14 ksi, with a question mark to indicate that Code 1, Fig. 1-9.1 indicates that high-strength steel is 20/12.5 = 1.6 times as strong as low-strength steels at 10^6 cycles.

The relative values of S_e in Table 3 for ferritic and 304 austenitic steels is worthy of comment in view of Appendix C, which indicates that girth butt welds in carbon steel pipe are at least as good as girth butt welds in type 304 stainless pipe. Unfortunately, the data in Appendix C are for relatively low-cycle and do not resolve the S_e question. Reference 7 gives results of resonance bending tests on pipe and girth butt welds in the pipe. These results indicate that girth butt welds in type 304 stainless steel pipe are slightly (10 to 20%) stronger than girth butt welds in carbon steel pipe, contrary to the data in Appendix C, but not by the factor of 27.2/14 = 1.94 indicated by the ratios of S_e in Table 3.

It is apparent from the preceding discussion that considerable uncertainty exists concerning an appropriate value for the endurance range limit S_e for evaluation of high-cycle fatigue of piping components. However, to the extent that the S_e estimates are valid, Table 3 indicates that (1) Code 1, using $2S_a$ at 10^6 cycles for S_e, is unconservative; and (2) Code 2 is unconservative for ferritic materials and also for austenitic materials if S_s is taken as zero.

6. TEES*

In addition to the differences between Codes 1 and 2 fatigue evaluation methods discussed in the preceding, there is a difference in the way stresses are calculated for tees. In Code 1 analysis, the stress range caused by a set of moment ranges as defined in Fig. 6 is calculated by:

$$S_n = K_{nb}C_{nb}M_b/Z_b + K_{nr}C_{nr}M_r/Z_r \ . \tag{27}$$

---

*The term "Tees" used here includes fabricated branch connections and ANSI B16.9 manufactured tees.

ORNL-DWG 83-4600 ETD

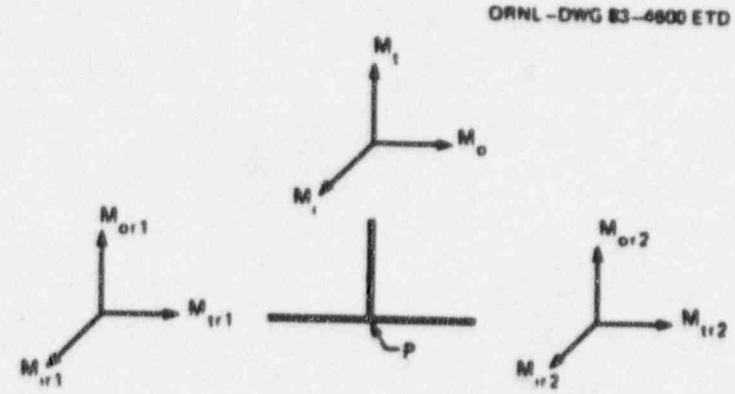

CODE 1

$M_b = (M_o^2 + M_i^2 + M_t^2)^{1/2}$,
$M_r = (M_{or}^2 + M_{ir}^2 + M_{tr}^2)^{1/2}$.

IF M_{ii1} AND M_{ii2} HAVE DIFFERENT SIGNS,
THEN M_{ii} IS THE SMALLER OF M_{ii1} AND M_{ii2}.
IF M_{ii1} AND M_{ii2} HAVE THE SAME SIGNS,
THEN M_{ii} = 0 WHERE ii = or, ir, OR tr.

CODE 2

EACH END OF THE TEE IS EVALUATED SEPARATELY, WITH:

$M_b = (M_o^2 + M_i^2 + M_t^2)^{1/2}$,
$M_{r1} = (M_{or1}^2 + M_{ir1}^2 + M_{tr1}^2)^{1/2}$,
$M_{r2} = (M_{or2}^2 + M_{ir2}^2 + M_{tr2}^2)^{1/2}$.

Fig. 6. Definition of moments for tees and code methods for calculating M_b, M_r, M_{r1}, and M_{r2}.

In Code 2 analysis,

$$S_2 = \text{maximum of } i(t/T)\,M_b/Z_b,\ iM_{r1}/Z_r,\ iM_{r2}/Z_r\ . \tag{28}$$

Equations (27) and (28) should not give the same calculated stresses, but from the standpoint of fatigue evaluation, they should give equivalent results. That equivalence, on an individual moment basis, is expressed by $2i = C_2K_2$. As will become apparent in the following paragraphs, this equivalence does not exist for some moment combinations.

The definition of M_r (Fig. 6) is such that M_r may be zero for one set of moments in the same direction (e.g., M_o, M^r_{tr1}, and M_{tr2}) but nonzero for another set of moments in the same direction (e.g., M_i, M_{ir1}, and M_{ir2}). Accordingly, to make comparisons between Codes 1 and 2, it is necessary to examine the three sets of moments in the same direction. Those three sets of moments are identified as M_1, M_2, and M_3, where M_1 and M_2 are the moments on the run, and M_3 is the moment on the branch. Equations (27) and (28) can be expressed as:

$$S_{1p} = Q_b|M_3|/Z_b + Q_rM_r/Z_r\ . \tag{29}$$

and

$$S_{2p} = \text{maximum of } Q_b|M_3|/Z_b,\ Q_r|M_1|/Z_r,\ \text{or } Q_r|M_2|/Z_r\ . \tag{30}$$

where $Q_b = K_{2b}C_{2b}$ or $2it/T$, $Q_r = K_{2r}C_{2r}$ or $2i$. A letter "p" has been added to the subscripts of S_1 and S_2 to emphasize that the stresses obtained by Eqs. (29) and (30) are only part of S_1 and S_2; the other two sets of same-direction moments must also be evaluated.

If the signs of M_1 and M_2 are the same, then $M_r = 0$ and Eq. (29) gives $S_{1p} = Q_b|M_3|/Z_b$. To show that Code 2 S_{2p} is the same as S_{1p}, we first note that, from static equilibrium, $M_3 = -(M_1 + M_2)$; hence, $|M_3| \geq |M_2|$ and $|M_3| \geq |M_1|$. We then introduce the parameter Z':

$$Z' = Z_bQ_r/(Z_rQ_b)\ . \tag{31}$$

and note that $Z' \leq 1.0$, because $Z_b \leq Z_r$ and $Q_r \leq Q_b$. If $Z' \leq 1$, then $Q_r|M_1|/Z_b$ and $Q_r|M_2|/Z_r$ will be less than $Q_b|M_3|/Z_b$ and Eq. (30) will give $S_{2p} = Q_b|M_3|/Z_b = S_{1p}$. Accordingly, the nonequivalence between Codes 1 and 2 occurs *only* if the signs of M_1 and M_2 are different.

For M_1 and M_2 with different signs, we take $|M_2| \geq |M_1|$. Then $M_r = |M_1|$ and $|M_3| = |M_1 + M_2|$. Equation (30) becomes:

$$S_{2p} = \text{maximum of } Q_b|M_3|/Z_b \text{ or } Q_r|M_2|/Z_r\ . \tag{32}$$

The ratio of S_{1p}/S_{2p} can then be calculated by:

$$S_{1p}/S_{2p} = \text{lesser of } (A - M')/A \text{ or } A - M' \ . \tag{33}$$

If $M' = M_1/M_2$, then M' is negative and varies between 0 and -1, and

$$A = (M' + 1)/Z' \ .$$

For any M' between 0 and -1, there is a maximum in S_{1p}/S_{2p} given by

$$(S_{1p}/S_{2p})_{max} = 1 - M' \text{ at } Z' = 1 + M' \ . \tag{34}$$

Noting that M' approaches -1 as $Z' \rightarrow 0$ for a small branch in a large run, Eq. (34) indicates that the nonequivalence between Codes 1 and 2 can be as much as a factor of 2 with Code 1 always being more conservative than Code 2.

Which is more accurate, Code 1 or Code 2? In a physical sense, Code 1 implies that the stress caused by M_3, reacted by either M_1 or M_2, adds to the stress caused by M_1 reacted by M_2. This is probably too conservative; it implies that the maximum stress caused by the two sources are at the same point and in the same direction. Code 2, on the other hand, implies that the stresses caused by the two sources do not add to each other at all.

The preceding discussion, in which it was shown that Code 1 might be more conservative than Code 2 by as much as a factor of 2, was based on the equivalences $Q_b = K_{sb}C_{sb} = 2i(t/T)$ and $Q_r = K_{sr}C_{sr} = 2i$. However, this equivalence does not exist for run moments on fabricated tees. The difference is illustrated by the following example.

Consider a 24-in.-OD by 0.375-in. nominal wall run pipe with a 1.315-in.-OD by 0.133-in. nominal wall drain connection. There are no moments on the drain; hence, S_s will be controlled by $iM_{r1}/Z_r = iM_{r2}/Z_r$. The value of i is $0.9\,(R/T)^{2/3} = 8.98$. For Code 1, because M_{r1} and M_{r2} have the same signs, $S_1 = C_{sr}K_{sr}M_{r1}/Z_r = C_{sr}K_{sr}M_{r2}/Z_r$. The value of C_{sr} is $1.15\,[(R/T)(r/R)/(t/T)]^{1/4} = 1.67$; the value of K_{sr} is 1.75, giving $K_{sr}C_{sr} = 2.92$. In this example, $2i$ is equal to $6.15\,C_{sr}K_{sr}$; hence, Code 2 is far more conservative than Code 1.

7. CODE 2 COVERAGE OF LOADINGS OTHER THAN MOMENTS

As noted in Chap. 1 and several other places in the preceding text, Code 2 covers only moment loading. However, as also noted in Chap. 1, no fatigue analysis is required for Class 2 or 3 vessels, pumps, or valves, and in this sense, Code 2 is more complete than required for other Class 2 or 3 components. Despite the preceding sentence, which might be taken as indicating that Code 2 is sufficiently complete, in this chapter we discuss the extent that the present rules cover cyclic pressure and thermal gradients and proceed with an exploratory discussion of how Code 2 might be extended to more explicitly cover loadings other than moment loadings.

The significance of S_s in Eq. (6) was discussed in Sect. 4.6, where it was concluded that S_s in a fatigue evaluation does not make much sense as a mean stress. Rather, S_s appears to serve as an allowance for cyclic loadings other than cyclic moments.

7.1 Allowance for Cyclic Pressure

The equation for S_s explicitly includes pressure loading in the form $S_{sp} = pd^2/(D^2 - d^2)$, where p = internal pressure, d = pipe ID, and D = pipe OD. Considering the crude approximations involved in its use, S_{sp} might well be calculated by the simpler form used in Eq. (14), $S_{sp} = pD_o/4T$, where D_o = outside diameter of pipe and T = nominal wall thickness of pipe. However, the significant aspect here is that S_s includes the axial stress caused by internal pressure in (capped) straight pipe. As a bound, we will examine the question: Is $S_s \leq S_h$ sufficient to guard against fatigue failure caused by cyclic pressure?

The most sensitive piping product to cyclic pressure is usually branch connections or tees. Code 1 gives C_1 and K_1 stress indexes such that the C_1K_1 product is unlikely to exceed 6. This means that the maximum peak stress S_p is not likely to exceed 12 times $pD_o/4T$. If S_h = 15 ksi (SA106 Grade B up to 650°F) and p is such that $pD_o/4T$ = 7.5 ksi corresponding to the maximum allowable hoop stress of 15 ksi for pressure design, then $S_p = 12 \times 7.5 = 90$ ksi range. From Eq. (24), it can be seen that a peak stress range of 90 ksi corresponds to an allowable N of ~5000 cycles. Accordingly, it appears the $S_s = S_h$ contains an allowance for cyclic pressure loading of ~5000 cycles from zero to the maximum permissible design pressure and back to zero. If S_s includes significant weight stresses and the weight (fluid contents) is constant, then an additional margin is provided for cyclic pressures.

For other material and temperatures, the allowance for cyclic pressure would vary with the value of S_h; for example, for SA106 Grade C up to 650°F, S_h = 17.5 ksi, $S_p = 6 \times 17.5 = 105$ ksi, and N [by Eq. (24)] is $(490/105)^5$ = 2200 cycles from zero to the maximum design pressure and back to zero.

7.2 Allowance for Thermal Gradients

The equation for S_s does not include thermal gradients analogous to the last three terms in Eq. (2). However, as indicated in Fig. 3, there is a margin for thermal gradients up to N of about 7000. For example, at N = 100 of both moment and pressure cycles, the margin between Eq. (24) and the line identified as $S_s = 0$ is $490/100^{0.2} - 1.25(15 + 15) = 158$ ksi. This margin, for example, would provide an allowance for the ΔT_2 thermal gradient term of Eq. (2), occurring 100 times, of:

$$\Delta T_2 = 158{,}000 \times (0.7/180) = 614°F ,$$

where $(1 - \nu) = 0.7$ and $E\alpha = 180$ psi/°F. Of course, for larger numbers of cycles (either of moment, pressure, and thermal gradients simultaneously or independently), the available margin for thermal gradients becomes smaller and essentially vanishes at and above 7000 cycles of moment and/or pressure cycles.

7.3 Use of Eq. (2) for Combined Loadings

This section, and the following Sect. 7.4, contains an exploratory discussion of how Code 2 fatigue evaluation could be improved in completeness and consistency. Firm recommendations would require further study of such aspects as the difference between Codes 1 and 2 in the evaluation of tees, appropriate values of S_e, and the validity of assumptions involved in the following discussion.

Code 2 fatigue evaluation could be improved in completeness and consistency by (1) calculating S_E by Eq. (2) and (2) limiting S_E by Eq. (24). This, in effect, assumes that the relationship $2i = C_2K_2$ is more generally valid (i.e., $2i = C_1K_1 = C_2K_2 = C_3K_3$). The advantages of this approach, as compared with a Code 1 fatigue evaluation, are that there is no need to calculate S_n separately and the K_e adjustment is not needed.

There are test data on piping products that could be used to examine the validity of $2i = C_1K_1$ for pressure loading. However, test data on piping products are not available for examining the validity of $2i = C_3K_3$ for thermal gradient loading. Also, no test data on piping products are available in which there were combinations of cyclic moments, pressure, or thermal gradients.

Equation (2) involves the implied assumption that maximum stresses caused by pressure, moments, and thermal gradients occur at the same location in a piping product, and in a direction so that they add to each other to form the total stress. In Sects. 7.1 and 7.2, that tacit assumption was also made.

In the case of combined pressure and moment loading on branch connections or tees, usually the stress caused by pressure is relatively low at the location of maximum stress caused by moment; and vice versa. Accordingly, the assumption of stress coincidence may contain significant conservatism. However, in the case of a girth butt weld in straight pipe, the axial stress adds directly to the moment stress. Similarly, thermal gradient stresses may or may not be coincident with locations of maximum stresses caused by pressure and/or moment.

7.4 Code 2 Cumulative Usage Equation

The Code 2 cumulative damage rule is discussed at the end of Chap. 3 [see Eq. (13)]. If Code 2 were changed along the lines suggested in Sect. 7.3, a corresponding cumulative damage rule could be

$$N = N_r + \sum_{i=1}^{i=k} (S_i/S_r)^5 N_i \, , \tag{35}$$

where

- N = total number of anticipated cycles in operation, which determines the value of the stress range reduction factor f in Eq. (6);
- N_r = number of anticipated cycles of an arbitrarily selected particular load cycle with a calculated stress range S_r;
- N_i = number of anticipated cycles with the stress range S_i.

If S_r or S_i is less than twice S_e, then N_r or N_i may be taken as zero. For fatigue evaluation acceptability, Eq. (36) must be satisfied:

$$N \leq (490/S_r)^5, \text{ with } S_r \text{ in ksi} \, . \tag{36}$$

Values of S_e would have to be included in Code 2. S_r and S_i would be calculated by Eq. (2).

The following example illustrates the procedure. Assume S_e = 14 ksi, S_r = 50 ksi, N_r = 200, and the following values for S_i and N_i:

Cycle type	S_i	N_i
1	130	100
2	90	400
3	40	6000
4	13	10^9

For this example,

$$N = 200 + (130/50)^5 \times 100 + (90/50)^5 \times 400 + (40/50)^5 \times 6000 + (13/50)^5 \times 0,$$

$$N = 200 + 11881 + 7558 + 1966 + 0 = 21605.$$

From Eq. (36), $(490/50)^5$ = 90390, and because 21605 < 90390, the particular piping product involved in this example would be acceptable from a fatigue evaluation standpoint.

7.5 Primary Stress Protection, High Temperatures

Throughout this report, and particularly in Sects. 7.3 and 7.4, the focus has been on fatigue evaluations. Note that Code 2, NC/ND-3640, contains rules for pressure design and nothing in this report is intended to suggest any changes in NC/ND-3640. Code 2 (Winter 1981 Addenda) Eqs. (8) and (9) function to avoid gross plastic deformations under combined pressure and moment loads, using the B_1 and B_2 indexes. No change in these Code 2 equations is intended by this report. Indeed, with the potential changes discussed in 7.3, Code 2 Eqs. (8) and (9) become even more significant and may often be the controlling factor rather than the fatigue evaluation.

Industrial piping codes (e.g., ANSI B31.1 and B31.3) cover temperatures higher than 700°F for ferritic steels and 800°F for austenitic steels and other high alloys. The suggestion in Sect. 7.3 involves the implicit assumption that Eq. (24) is valid for all materials and temperatures up to 700 or 800°F for stresses down to S_e. This assumption is not valid for higher temperatures, hence industrial piping codes should *not* follow the suggestion in Sect. 7.3 for all of their temperatures. Also, industrial piping codes would have to make sure they have adequate protection against gross plastic deformations equivalent to Code 2 Eqs. (8) and (9).

8. SUMMARY

8.1 Chapters 2–4, Fatigue Evaluation up to 10^6 Cycles

Considering the entirely different approaches used in Codes 1 and 2, the agreement between the two approaches is gratifyingly good. The K_e factor is mainly responsible for this relatively good agreement. However, Code 2 appears to be potentially unconservative for high-strength materials like SA672-J100. Code 1 appears to be potentially unconservative for type 304 material for $N \geq 10^4$, $K_2 = 2$, and for $N \geq 10^5$, $K_2 = 1$.

8.2 Chapter 5, High-Cycle Fatigue

Both Code 1 (using S_a at 10^6 cycles as an endurance limit amplitude) and Code 2 (using S_E with $f = 0.5$) appear to be potentially unconservative for evaluation of accumulated cycles of about 10^7 or more. Table 3 shows our estimated value of S_e (endurance limit range) for an effectively infinite number of cycles.

8.3 Chapter 6, Tees

Stresses in tees are evaluated differently in Codes 1 and 2. Under certain combinations of moments, Code 1 can be more conservative than Code 2 by a factor of up to 2. However, for evaluating stresses caused by run moments, Code 2 can be much more conservative than Code 1.

8.4 Chapter 7, Loadings Other than Moments

Chapters 2–6 are concerned with correlations between fatigue evaluation for moment loadings, because Code 2 explicitly covers only moment loadings. It appears that Code 2 rules, as presently written, have a substantial allowance for cyclic pressure and, for a low number of design cycles (e.g., 100), a substantial allowance for thermal gradients.

In Sects. 7.3 and 7.4, exploratory comments and suggestions are given concerning Code 2 modifications that would explicitly cover pressure and thermal gradients as well as moments. The major additional work involved in routine fatigue evaluations would consist of the determination of the thermal gradients, ΔT_1, ΔT_2, T_a, and T_b. In Sect. 7.5, note is made that this report is concerned with fatigue evaluation and that Code rules for pressure design and Code equations for protection against gross plastic deformation must be observed as well.

REFERENCES

1. A. R. C. Markl, "Fatigue Tests of Welding Elbows and Comparable Double-Miter Bends," *Trans. ASME* 69, 869–79 (1947).

2. A. R. C. Markl and H. H. George, "Fatigue Tests on Flanged Assemblies," *Trans. ASME* 72, 77–87 (1950).

3. A. R. C. Markl, "Fatigue Tests of Piping Components," *Trans. ASME* 74, 287–303 (1952).

4. S. W. Tagart, "Basis for Paragraph NB-3228.3 of ASME Section III Simplified Elastic-Plastic Analysis," April 16, 1976.

5. A. R. C. Markl, "Piping Flexibility Analysis," *Trans. ASME* 77, 419–41 (1955).

6. R. P. Newman, "The Influence of Weld Faults on Fatigue Strength with Reference to Butt Joints in Pipe Lines," *Trans. Inst. Mar. Eng.* 168, 153 (1956).

7. W. G. O'Toole and E. C. Rodabaugh, *Fatigue Tests on 4" Std. Wt. Carbon and Stainless Steel Pipe and Circumferential Butt Weld Joints*, Tube Turns, Louisville, Ky., Report No. 8.031 (October 1961).

8. R. P. Meister et al., *Effects of Weld-Joint Imperfections on Piping Performance*, Battelle Memorial Institute (July 31, 1964).

9. M. G. Dawes, "Fatigue Strength of Tubes Butt Welded Using a Ceramic Coated Backing Member," *Br. Weld. J.* 14, 304–12 (1967).

10. D. E. Hardenbergh, S. Y. Zamrick, and A. J. Edmondson, "Experimental Investigation of Stresses in Nozzles in Cylindrical Pressure Vessels," *Weld. Res. Counc. Bull.* 89 (July 1963).

11. A. G. Pickett et al., *Low Cycle Fatigue of One-Half Scale Model Pressure Vessels*, Progress Reports Nos. 9–12, Southwest Research Institute, San Antonio, Tex. (July 1964–January 1965).

12. T. Forte and C. E. Jaske, *Fatigue Evaluation of 14x6 Insert Weldolet Branch Connections in Carbon Steel Pipe*, Battelle-Columbus Report to Bonney Forge, Allentown, Pa., April 30, 1981.

13. R. A. Weed and N. E. Johnson, *Experimental Stress Analysis and Fatigue Test of ANSI Standard B16.9 Tees*, ORNL-Sub-4356 (undated draft).

14. J. K. Hayes and B. Roberts, "Experimental Stress Analysis of 24-in Tees (T10)," *Trans. ASME, J. Eng. Ind.*, pp. 919–28 (November 1971).

15. J. K. Hayes and S. E. Moore, "Experimental Stress Analysis for Four 24-in ANSI Standard B16.9 Tees (T11, T12, T13, T16)," *Trans. ASME, J. of Pressure Vessel Technology*, pp. 537–52 (November 1977).

16. E. C. Rodabaugh and S. E. Moore, *Comparisons of Test Data with Code Methods of Fatigue Evaluation*, ORNL/TM-3520 (November 1971).

17. M. E. Mayfield, E. C. Rodabaugh, and R. J. Eiber, *Relevance of Fatigue Tests to Cold Leg Piping*, NUREG/CR-0325 (September 1978).

18. J. D. Heald and E. Kiss, *Low Cycle Fatigue of Prototype Pipe Components*, General Electric (San Jose) Report GEAP-10763 (January 1973).

19. E. Kiss, J. D. Heald, and D. A. Hale, *Low-Cycle Fatigue of Prototype Piping*, General Electric (San Jose) Report GEAP-10135 (January 1970).

20. J. D. Heald and E. Kiss, "Low Cycle Fatigue of Nuclear Pipe Components," *Trans. ASME, J. of Pressure Vessel Technology* 96(3), 171–76 (August 1974).

21. J. S. Blair, "Reinforcement of Branch Pieces," *Engineering*, London (1947).

22. E. J. Mills, T. J. Atterbury, and G. M. McClure, *AGA Project NG-11, Study of Effects of Cyclic Bending Loads on Performance of Branch Connections*, Battelle-Columbus Report to American Gas Association (May 1962).

23. T. R. Gurney and S. J. Maddox, "A Re-Analysis of Fatigue Data for Welded Joints in Steel," *Weld. Res. Int.* 3(4), 1–54 (1973).

24. National Research Institute for Metals, Tokyo, Japan, "NRIM Fatigue Data Sheet No. 5, Data Sheets on Fatigue Properties for Butt-Welded Joints of SM50B High Tensile Structural Steel Plates," 1978.

25. B. Pollard and R. J. Cover, "Fatigue of Steel Weldments," *Weld. Res. Supplement* (November 1972).

Appendix A

BACKGROUND OF THE K_e FACTOR

The purpose of the $3S_m$ limit on the range of primary-plus-secondary stress S_n is to ensure the validity of the S_a value used in the fatigue evaluation. Conceptually, the limit is the shakedown limit of $2S_y$ because $S_m = (2/3)S_y$ and $3S_m = 2S_y$. Actually, for most materials and temperatures, the value of S_m is *not* $(2/3)S_{yc}$, where S_{yc} is the Code-tabulated or expected (at temperatures above room temperature) minimum yield strength. Examples are (1) S_m for SA106 Grade B at 100°F = 20 ksi, S_{yc} = 35 ksi, $S_m = 0.57\ S_{yc}$; and (2) S_m for SA312 type 304 at 500°F = 17.5 ksi, S_{yc} = 19.4 ksi, $S_m = 0.90\ S_{yc}$.

The shakedown criteria of $S_n \leq 2S_y$ are based on an idealized, elastic perfectly plastic material; most piping materials are not really such idealized materials. Furthermore, S_{yc} is a minimum; typical yield strengths are about 20% higher than S_{yc}. Therefore, it is apparent that the $3S_m$ limit is only a rough approximation of the shakedown limit.

Prior to the start of work on Class 1 piping for ANSI B31.7, a simple procedure for fatigue evaluation when $S_n > 3S_m$ did not exist. Writers of ANSI B31.7, at that time, noted that:

1. Stresses caused by a linear through-the-wall temperature gradient ΔT_1 should be considered to be part of S_n. Indeed, in the Bree[1] shakedown evaluation, ΔT_1 is *the* source of bending stresses that, in combination with a membrane stress (e.g., from pressure), can cause cyclic plasticity or ratchetting.
2. Test data on piping products were available (e.g., Markl[3]) to clearly show that, even for $S_n > 3S_m$, the product could withstand a significant number of cycles without failure. Equation (24) of the text as applied to an elbow illustrates this. For an elbow, $K_2 = 1$; hence, $2iS_d$ is equivalent to S_n. With $2iS_d = S_n = 6S_m$ = 180 ksi, Eq. (24) gives N of 150 cycles; N_f = 32 x 150 = 4800 cycles.

Making ΔT_1 stresses part of S_n increased the frequency of $S_n > 3S_m$ in designed piping systems. Recognition that, even if $S_n > 3S_m$, significant fatigue cycles could be withstood motivated the development and acceptance of a "simplified elastic-plastic" evaluation procedure for $S_n > 3S_m$.

ANSI B31.7-1969 for $S_n > 3S_m$ required that:

$$S = C_2 M_i / Z \leq 3S_m , \tag{A.1}$$

where M_i was the resultant moment range caused by restraint of thermal expansion. If Eq. (A.1) was met, then:

$$S_{alt} = (1/2)[S_p + A(S_p - S_n)](S_n/3S_m) \; . \tag{A.2}$$

where S_{alt} was the calculated stress amplitude to be used to enter the Code design fatigue curves. The value of A was obtained from ANSI B31.7 Fig. D-201, included here as Fig. A.1. The use of Eq. (A.2) was restricted to <250 cycles of $S_n > 3S_m$. Tagart[3] discusses the development

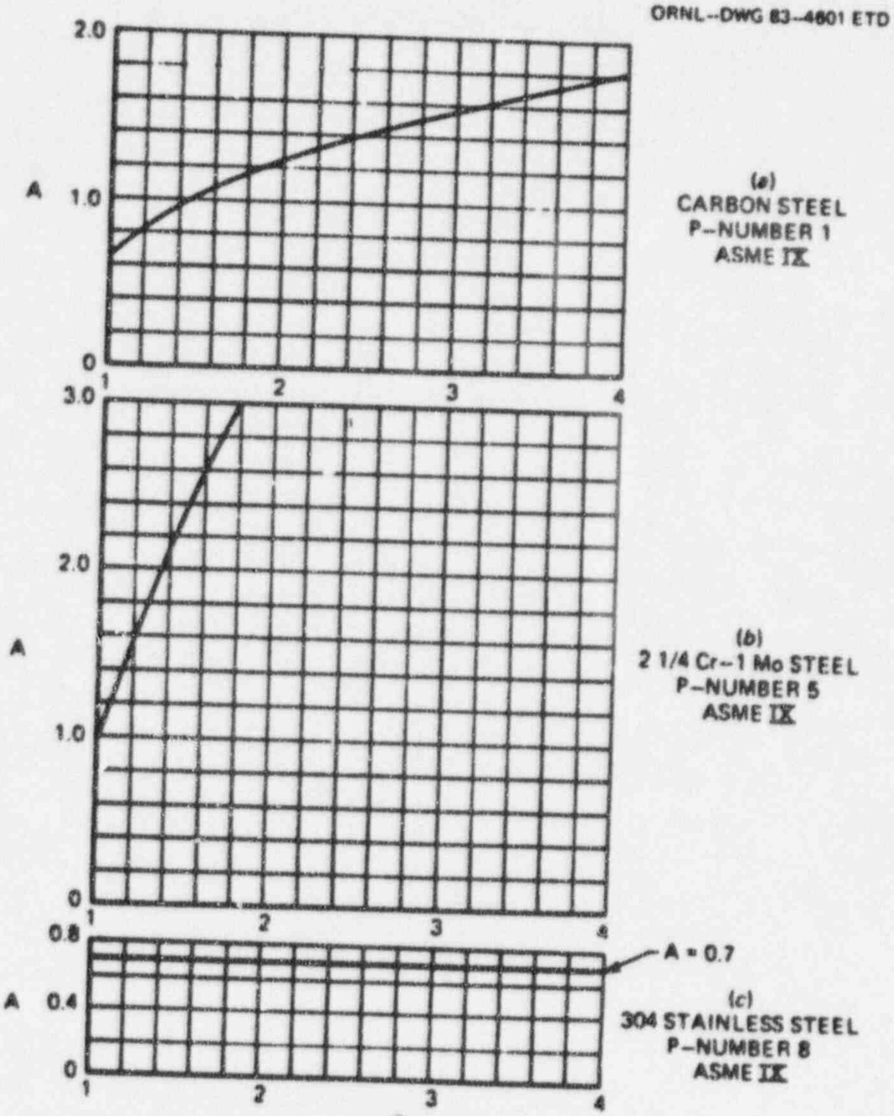

Fig. A.1. *A*-factors for use in Eq. (A.2). *Source*: American Society of Mechanical Engineers, *Nuclear Power Piping*, USAS B31.7-1969.

of Eq. (A.2) and the 250-cycle limit. The basis for Eq. (A.1) is more nebulous; it came in large part from the desire to limit expansion stresses to the same "ball park" as those permitted in industrial piping codes.

Code Case 1441, "Waiving of $3S_m$ Limit for Section III Construction," was published in 1970. It gave rules that are almost the same as those now in Code 1 (see Chap. 2 of the text). Two exceptions were: (1) the number of cycles with $S_n > 3S_m$ was limited to 1000, (2) the value of n, for austenitic stainless steels, was 0.5 rather than the present $n = 0.3$.

Table A.1 shows comparisons between Code Case 1441 (1970) and Code 1 (1980) for stainless steels; Case 1441 uses $n = 0.5$ rather than the present $n = 0.3$. It can be seen that use of $n = 0.5$ gives very high allowable fatigue design stresses for low cycles; the $n = 0.5$ was soon (1971) changed to its present value of 0.3.

Table A.2 shows comparisons between ANSI B31.7-1969 and Code 1. Considering the order of accuracy involved, the method used in ANSI B31.7-1969 for fatigue evaluation for $S_n > 3S_m$ is equivalent to the K_e factor used in Code 1.

Tagart[4] has prepared a description of the basis for the K_e factor. Because, to our knowledge, it has not been published and because questions regarding the basis for the K_e factor frequently arise, Tagart's discussion is quoted in full in the following paragraphs. In addition

Table A.1. Comparisons of allowable values of S_p (ksi), Code Case 1441 and Code 1

N	SA312 type 304 at 100°F			
	$K_2 = 1$		$K_2 = 2$	
	Case 1441	Code 1	Case 1441	Code 1
10	650^a	390^a	650^a	390^a
10^2	240^a	144^a	240^a	179
10^3	109^a	87.1	155	140
10^4	80.0	71.6	118^b	118^b
10^5	65.8	63.3	75.0^b	75.0^b
10^6	52.0^b	52.0^b	52.0^b	52.0^b

[a]Indicates that $S_n > 3mS_m$, $K_e = 1/n$, $S_p = 2nS_a$.

[b]Indicates that $S_n < 3S_m$, $K_e = 1.0$, $S_p = 2S_a$.

Table A.2. Comparisons of allowable values of S_p (ksi), ANSI B31.7-1969 and Code 1

N	SA106 Grade B at 100°F				SA312 type 304 at 100°F			
	$K_s = 1$		$K_s = 2$		$K_s = 1$		$K_s = 2$	
	B31.7	Code 1	B31.7	Code 1	B31.7	Code 1	B31.7	Code 1
10	264	232[a]	288	296	279	390[a]	340	390[a]
10^2	157	127	181	190	170	144[a]	207	179
10^3	99.8	87.0	121	134	114	87.1	139	140
10^4	67.3	65.0	76.0[b]	76.0[b]	84.1	71.6	118[b]	118[b]
10^5	40.0[b]	40.0[b]	40.0[b]	40.0[b]	67.1	63.3	75.0[b]	75.0[b]
10^6	25.0[b]	25.0[b]	25.0[b]	25.0[b]	52.0[b]	52.0[b]	52.0[b]	52.0[b]

[a]Indicates that $S_n > 3mS_m$, $K_e = 1/n$, $S_p = 2nS_a$.

[b]Indicates that $S_n < 3S_m$, $K_e = 1.0$, $S_p = 2S_a$.

to the references cited by Tagart, Refs. 5 and 6 contain more extensive and direct correlations between fatigue tests on piping products and the Code 1 with K_e method of fatigue evaluation.

BASIS FOR PARAGRAPH NB 3228.3 OF ASME SECTION III SIMPLIFIED ELASTIC-PLASTIC ANALYSIS*

The rules currently appearing in the ASME Section III Code concerning simplified elastic-plastic analysis have their origin in the development of detailed stress analysis for nuclear power piping components under the former USAS B31.7 Nuclear Power Piping Code. In the process of developing that code, the frequently occurring large primary plus secondary stresses which result in piping components gave need for a simplified procedure to evaluate these effects. A detailed procedure was implemented into the B31.7 code and referenced by Paper 68-PVP-3, listed as Reference 1 [Ref. 3 of this Appendix]. This development relied on tests of notched bar specimens which measured the strain concentrating effect when the $3S_m$ limit was exceeded. Although it was generally agreed

*Original text by S. W. Tagart.

that the recommended procedures presented in this paper were safe and conservative by those who reviewed them in detail, further developments of simplified formulas occurred when the piping code was combined into ASME Section III. Due to the complexity of the elastic-plastic behavior, no simple formula could be developed which would accurately represent everything which goes on.

In simple terms, the strain concentration phenomena which occurs is illustrated by Figure 1 [Fig. A.2 of this Appendix]. Here we see a plot of the peak strain concentration factor in either a notched member or a member with some other type of stress concentration. The peak strain concentration remains constant from O to A where the material behavior is perfectly elastic. At Point A, the strain concentration begins to exceed the elastic stress concentration, K_t, and continues to rise until some Point B is reached at which a maximum strain concentration occurs.

If deflection is continued, the strain concentration begins to drop off as shown by Point C. Langer, in Reference 2 [Ref. 7 of this Appendix], has estimated the generalized maximum strain concentration which can occur at a point such as B. He illustrates that the strain concentration factor K_E is approximately 1/n, where n is the strain hardening exponent of the material. This maximum value of strain concentration is the basis for the assumed shape of the K_E correction factor which appears in the Code. The specific Code formula shown here as equation 1 which quantitatively expresses this strain concentration, contains two material terms, n and m. The m term was introduced into the formula in order to produce any

ORNL-DWG 83-4607 ETD

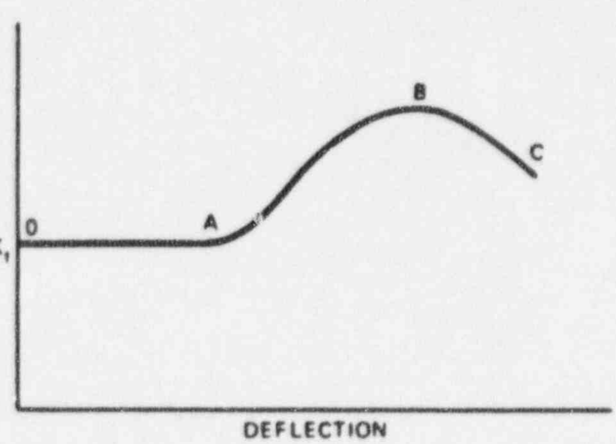

Fig. A.2. Schematic illustration of peak-strain concentration in a notched beam as a function of deflection. *Source*: Ref. 4.

desired slope on the K_E factor in region A of Figure 2 [Fig. A.3 of this Appendix]. Thus, the form of equation 1 was selected in order to provide two features: 1) a maximum correction for the strain concentration of 1/n and 2) any experimentally observed slope of the K_E correction in region A. While the strain hardening exponent n is easily obtained for the static case by measuring the uniform elongation at maximum load during the tensile test, such values of n may not reflect accurately the behavior which occurs in a fatigue situation. Therefore, the values of n which appear in the code for this procedure are only approximate values of the strain hardening exponent as compared with those from a tensile test. There is no straightforward method for measuring m without using the results of fatigue tests. The method which was used to establish the validity of the correction factor K_E supplied by equation 1 for specific m and n values was through comparison with fatigue test results. Other methods are possible, but a standard method has not been developed at the present time. Numerous fatigue tests have been run and the results of these tests have been published and have demonstrated that the correction predicted is conservative for use with the Code.

References 3 through 8 [Refs. 7–13 of this Appendix] illustrate some of the sources of verifying the current elastic-plastic design formulas. For example, Figure 15 of Reference 8 [Ref. 13 of this Appendix] shows a direct comparison between

ORNL–DWG 83–4603 ETD

$$
(1)\quad \begin{cases} K_E = 1.0 & (S_n < 3S_m) \\ K_E = 1.0 + \dfrac{1-n}{n(m-1)}\left(\dfrac{S_n}{3S_m} - 1\right) & (3S_m < S_n < 3_m S_m) \\ K_E = 1/n & (S_n > 3_m S_m) \end{cases}
$$

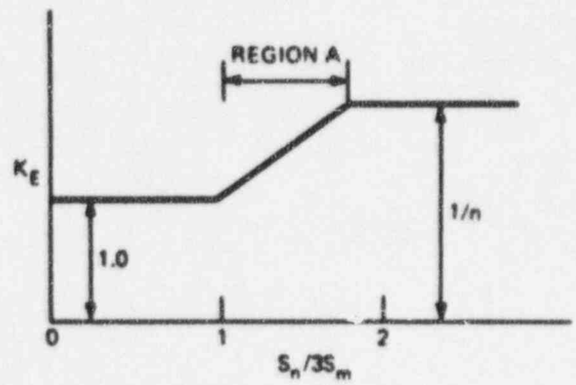

Fig. A.3. Schematic illustration of the variation of K_e as a function of primary-plus-secondary stress. *Source*: Ref. 4.*

the strain concentration factors used in the Code and the values obtained from tests on type 304 stainless steel. In the original concept of the elastic-plastic correction as presented in Reference 1 [Ref. 3 of this Appendix], a limit of 250 cycles is suggested below which no specific account was required to assure that ratcheting would be negligible. The current rules of ASME Section III have no such limitations; however, it should be noted that in NB3223.3, Paragraph (a), a range of primary plus secondary membrane bending stress intensity excluding thermal bending stresses must always be less than $3S_m$.

Paragraph (d) requires that the through wall thermal gradient effects meet the requirements of NB 3222.5 for ratcheting due to pressure and thermal effects. In addition, the conservative values of the K_E factor drastically reduces the allowable fatigue life cycles. Satisfying these requirements provides assurance that a negligible amount of ratcheting can occur, therefore, no additional requirement for limiting cycles due to ratcheting is necessary.

References

1. J. Bree, "Elastic-Plastic Behavior of Thin Tubes Subjected to Internal Pressure and Intermittent High-Heat Fluxes with Application to Fast-Nuclear Fuel Elements," *J. Strain Anal.* 2(3), 226–238 (1967).

2. A. R. C. Markl, "Fatigue Tests of Piping Components," *Trans. ASME* 74, 287–303 (1952).

3. S. W. Tagart, "Plastic Fatigue Analysis of Pressure Components," ASME Paper No. 68-PVP-3, pp. 209–226 in Vol. 1 of *ASME Pressure Vessels and Piping: Design and Analysis, A Decade of Progress*, New York, 1972.

4. S. W. Tagart, "Basis for Paragraph NB-3228.3 of ASME Section III Simplified Elastic-Plastic Analysis," April 16, 1976.

5. E. C. Rodabaugh and S. E. Moore, *Comparisons of Test Data with Code Methods of Fatigue Evaluation*, ORNL/TM-3520 (November 1971).

6. M. E. Mayfield, E. C. Rodabaugh, and R. J. Eiber, *Relevance of Fatigue Tests to Cold Leg Piping*, NUREG/CR-0325 (September 1978).

7. B. F. Langer, "Design-Stress Basis for Pressure Vessels," *Exp. Mech.* 84(3), 389–402 (January 1971).

8. E. Kiss, J. D. Heald, and D. A. Hale, "Low-Cycle Fatigue of Prototype Piping," General Electric (San Jose) Report GEAP-10135 (January 1970).

9. J. D. Heald and E. Kiss, "Low Cycle Fatigue of Nuclear Pipe Components," *Trans. ASME J. of Pressure Vessel Technology* 96(3), 171-176 (August 1974).

10. E. C. Rodabaugh, Phase Report No. 115-2 (February 1969).

11. T. L. Gerber, "Effect of Constraint and Loading Mode on Low-Cycle Fatigue Crack Initiation - Comparison with Code Design Rules," GEAP-20662 (October 1974).

12. T. Udoguchi and Y. Asada, "Initiation of Low Cycle Fatigue Strength of Piping Components," paper presented at Second International Conference on Pressure Vessel Technology, San Antonio, Texas, October 1973.

13. Y. Ando et al., "Low Cycle Fatigue Strength of Piping Components," paper presented at Second International Conference on Pressure Vessel Technology, San Antonio, Texas, October 1973.

Appendix B

BASIS OF CODE 1 FATIGUE DESIGN CURVES

Basic Test Data, Carbon and Low-Alloy Steels

Figure B.1 shows the basic data used to establish the design fatigue curve in Code Fig. I-9.1, UTS $\leq$ 80 ksi. Figure B.1 consists of Figs. 9 and 10 of the Criteria.[1] The data in Fig. B.1 are from strain-controlled, zero mean strain, fatigue tests of polished bars at (probably) room temperature. An equation of the form

$$S = [E/(4\sqrt{N_f})] \ln [100/(100 - A)] + B \qquad (B.1)$$

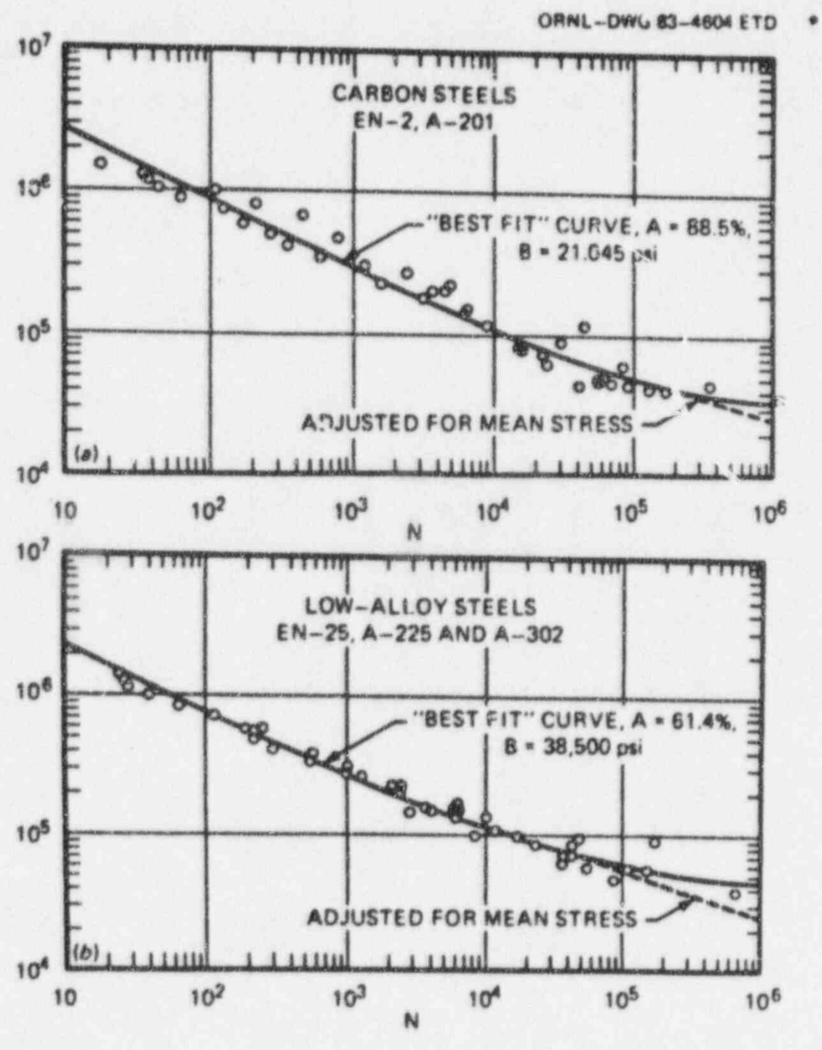

Fig. B.1. Basic test data: (*a*) carbon and (*b*) low-alloy steels. *Source*: Ref. 33.

was fitted to the average of the test data by selection of A and B. The percent reduction in area is sometimes used for A, but in general, A is simply a curve fitting parameter. The value of B is an endurance strength, that is, a value of S below which fatigue failure will not occur in a polished bar in dry air or equivalent environment. The design fatigue curve is obtained from Eq. (B.1) by: (1) applying an adjustment for mean stress effect, and (2) applying a factor of safety of 2 on stress or 20 on cycles, whichever gives the lower fatigue design stress.

Mean Stress Adjustment

Because of residual stresses at welds and other possible sources of mean stress such as installation misalignment in piping, the Code has taken the approach of adjusting the test results for the maximum possible effect of mean stress. The adjustment procedure is described in the Criteria.[8] The procedure is based on the Goodman diagram and the concept that the sum of the mean stress and reversed stress amplitude cannot exceed the yield strength of the material. The equivalent completely reversed stress S' is obtained by:

$$S' = S[(S_u - S_y)/(S_u - S)] \ , \quad \text{for } S < S_y \ ; \tag{B.2}$$

and

$$S' = S \ , \quad \text{for } S > S_y \ ; \tag{B.3}$$

where

S' = equivalent completely reversed stress amplitude,
S = reversed stress amplitude [Eq. (B.1)],
S_u = ultimate tensile strength of material,
S_y = yield strength of material.

To make the adjustment indicated by Eq. (B.2), values of S_u and S_y must be selected. These are not necessarily the minimum specified strengths, and a judgment must be made as to the appropriate values. The Criteria does not identify the values of S_u and S_y used to obtain the adjustments (dashed lines in Fig. B.1), but working backward, it appears that the following values were used.

	S_u	S_y
Carbon steels	80 ksi	40 ksi
Low-alloy steels	100 ksi	70 ksi

Having made the adjustment for mean stress, the design fatigue curve S_a

vs N is obtained by applying the factor of safety of 2 on stress or 20 on cycles.

The procedure described in the preceding paragraphs is illustrated in Table B.1. The value of the modulus of elasticity E was taken as 3×10^7 psi; this is the value shown in Code Fig. I-9.1. The value of E is significant in that stresses are equal to Ee, where e is the controlled strain. In principle, the value of E used in the analysis [e.g., to determine N_i in Eq. (1) of the text] should be the same as E used to develop the design fatigue curve. Alternatively, the design fatigue curves can be modified by multiplying the stresses in the curve by E'/E, where E' is the modulus used in the analysis. However, quite often the cycles occur over a range of temperatures, and part of a piping system may be at a different temperature than another part of the same system. Accordingly, an approximation of an appropriate E is often necessary. Fortunately, the variation of E with temperature over the range of temperature covered is relatively small and therefore is not a major source of uncertainty in a fatigue analysis.

It may be observed in Table B.1 that the Code-tabulated values of fatigue design stresses agree reasonably well with the average of the two sets of S_a. The Criteria states, "A single design curve is used for carbon and low-alloy steel below 80,000 psi ultimate tensile strength because . . . the adjusted curves for these classes of material were nearly identical."[1]

High-Alloy Materials

The Criteria[1] includes data for 18-8 stainless steels with an average-fit equation in the form of Eq. (B.1):

$$S = 8.4151 \times 10^6/\sqrt{N_f} + 43,500 \ , \qquad (B.4)$$

where $E = 2.6 \times 10^7$ psi (the value shown on Fig. I-9.2). The correspondence between the Criteria equation and Code-tabulated values is shown in Table B.2. Because S at 10^6 cycles is 51,915 psi, which was assumed to be greater than S_y, there is no mean stress correction in Code Fig. I-9.2. As can be seen in Table B.2, the values of S_a derived from Eq. (B.4) are in reasonable agreement with the Code-tabulated values.

Although the Criteria[1] gives data only for 18-8 stainless steels, the Code in its first (1963) edition indicated that Fig. I-9.2 was applicable to nickel-chrome-iron alloys. The present (1980) Code indicates that Fig. I-9.2 is applicable to austenitic stainless steels, nickel-chrome-iron alloy (e.g., SB167 Alloy 600), nickel-iron-chrome alloy (e.g., SB407 Alloy 800), and nickel-copper alloy (e.g., SB165 Alloy 400). The basis for including the other-than-austenitic steels in Fig. I-9.2 is not available.

About 1975, the need arose to extend the Code design fatigue curves to higher than 10^6 cycles. Jaske and O'Donnell[3] published the results of their review of fatigue test data on 300 series austenitic steels, nickel-

Table B.1. Illustration of method of developing design fatigue curves from completely reversed fatigue test data (stresses in ksi)

N	Carbon steel				Low-alloy steel				
	S[a]	S_{20}[b]	S'[c]	S_a[d]	S[e]	S_{20}[b]	S'[f]	S_a[d]	Code[g]
10	2761	634		634	2296	543		543	580
20	1959	455		455	1635	395		395	410
50	1247	296		296	1048	264		264	275
100	888	215		215	752	198		198	205
200	634	159		159	543	151		151	155
500	409	108		108	358	110		110	105
1000	296	82.9		82.9	264	89.0		89.0	83
2000	215	65.0		65.0	198	74.2		74.2	64
5000	144	49.0		49.0	139	61.1		61.1	48
1×10^4	108	41.0		41.0	110	54.5		54.5	38
2×10^4	82.9	35.3		35.3	89.0	49.8		44.5[h]	31
5×10^4	60.4	30.3		30.2[h]	70.4	45.6		35.2[h]	23
1×10^5	49.0	27.8		24.5[h]	61.1	43.5	47.1	23.5[h]	20
2×10^5	41.0	26.0		20.5[h]	54.5	42.1	36.0	17.9[h]	16.5
5×10^5	33.9	24.4	29.4	14.7[h]	48.6	40.8	28.4	14.2	13.5
1×10^6	30.3	23.6	24.4	12.2[h]	45.6	40.1	25.2	12.6[h]	12.5
1×10^7	24.4	22.3	17.5	8.77[h]					
1×10^8	22.5	21.8	15.7	7.83[h]					
1×10^9	21.9	21.7	15.1	7.55[h]					
1×10^{10}	21.7	21.7	14.9	7.46[h]					
1×10^{11}	21.7	21.7	14.9	7.43[h]					

[a] Equation (B.1) with $E = 3 \times 10^7$ psi, $A = 68.5$, $B = 21{,}645$ psi; $S = 8{,}664/\sqrt{N} + 21.645$ ksi.

[b] S_{20} = stress for N = 20 times value shown; that is, factor of safety of 20 on cycles.

[c] Equation (B.2) with $S_u = 80$ ksi, $S_y = 40$ ksi.

[d] S_a = lesser of $S/2$, S_{20}, or $S'/2$.

[e] Equation (B.1) with $E = 3 \times 10^7$ psi, $A = 61.4$, $B = 38{,}500$ psi; $S = 7{,}139/\sqrt{N} + 38.5$ ksi.

[f] Equation (B.2) with $S_u = 100$ ksi, $S_y = 70$ ksi.

[g] Value of S_a tabulated in Code 1, Table I-9.1 for Fig. I-9.1, UTS $\leq$ 80 ksi.

[h] Factor of safety of 2 on stress controls.

Table B.2. Comparisons of fatigue design stresses for 18-8 austenitic stainless steels (stresses in ksi)

N	S[a]	S_{20}[b]	S_a[c]	Code[d]	S_{aa}[e]	Proposed curve A[f]
10	2705	639	639	650		
20	1925	464	464	470		
50	1234	310	310	317		
100	885	232	232	240		
200	639	177	177	185		
500	420	128	128	136		
1000	310	103	103	109		
2000	232	85.6	85.6	89		
5000	163	70.1	70.1	70		
1×10^4	128	62.3	62.3	59		
2×10^4	103	56.8	51.5[g]	51		
5×10^4	81.1	51.9	40.6[g]	42.5		
1×10^5	70.1	49.5	35.1[g]	37.5		
2×10^5	62.3	47.7	31.2[g]	33.0		
5×10^5	55.4	46.2	27.7[g]	28.5		
1×10^6	51.9	45.4	26.0[g]	26.0	28.3[g]	28.3
2×10^6					26.9[g]	26.9
5×10^6					25.7[g]	25.7
1×10^7					25.1[g]	25.1
2×10^7					24.7[g]	24.7
5×10^7					24.3[g]	24.3
1×10^8					24.1[g]	24.1
1×10^9					23.8[g]	23.8
1×10^{10}					23.7[g]	23.7
1×10^{11}					23.7[g]	23.7

[a] Equation (B.1) with $E = 2.6 \times 10^7$, $A = 72.6$, $B = 43{,}500$ psi; $S = 8{,}415/\sqrt{N} + 43.5$ ksi.

[b] S_{20} = stress for N = 20 times value shown; that is, factor of safety of 20 on cycles.

[c] S_a lesser of S/2 or S_{20}.

[d] Value of S_a tabulated in Code Table I-9.1 for Fig. I-9.2.

[e] S_{aa} is S_a adjusted for $E = 2.83 \times 10^7$ psi.

[f] Proposed curve A (see text).

[g] Factor of safety of 2 on stress controls.

iron-chrome Alloy 800, nickel-chrome-iron Alloy 600, and nickel-chrome Alloy 718. One data point at 10^8 cycles was included. The high-stress data points were strain controlled; some of the low-stress data points were load controlled. Tests were run at various temperatures up to 800°F. According to Langer,[8] the Criteria data on 18-8 stainless steel included tests at temperatures up to 660°F.

The Jaske and O'Donnell paper gives separate curves in the form of Eq. (B.1) for the 300 series stainless steels, Alloy 800, Alloy 600, and Alloy 718. They found that the 300 series stainless steels, Alloy 800, and Alloy 600 could be grouped together for the purpose of design guidance. They then applied mean stress adjustment in the form of Eq. (B.2) with S_u = 94 ksi and S_y = 44 ksi. They used $E = 2.83 \times 10^7$ psi rather than $E = 2.6 \times 10^7$ psi as used in Code Fig. I-9.2. Numerical comparisons for the three materials and the combined three materials are shown in Table B.3.

For $N \leq 10^6$ cycles (present Code coverage), it can be seen in Table B.3 that the Jaske and O'Donnell design fatigue stresses are generally lower than the present Code (adjusted for $E = 2.83 \times 10^7$ instead of $E = 2.6 \times 10^7$). As an extreme example, for 300 series stainless steels at $N = 2 \times 10^4$ cycles, the Code allowable stress is 1.39 times the Jaske and O'Donnell best-fit curve. However, considering the conservatisms that usually exist in estimating the operating history and in calculation of stresses, this possible unconservatism is relatively small.

At present (July 1982), a proposed modification to Code Fig. I-9.2 is under consideration by the ASME Boiler and Pressure Vessel Committee. This proposal* maintains the present Code curve for $N \leq 10^6$ cycles. Above $N = 10^6$, three curves, identified as A, B, and C are proposed.

The A curve is simply an extrapolation of the present Code using the equation

$$S = (8415/\sqrt{N_f} + 43.5) \times (2.83/2.60) \ .$$

Values are shown in Table B.2 on the two right columns for $N \geq 10^6$.

The B curve is faired-in between the present Code stress at $N = 10^6$ and Jaske and O'Donnell "combined" curve, without any adjustment for mean stress.

The C curve is faired-in between the present Code stress at $N = 10^6$ and the Jaske and O'Donnell "combined" curve, with adjustment for the maximum effect of mean stress. A comparison is shown in Table B.3 on the two right columns for $N \geq 10^6$.

The question arises as to which of the three proposed curves is most appropriate for piping evaluation in conjunction with Eqs. (1) and (2) of the text. The question is not trivial because for $N = 10^8$, the C curve gives stresses that are ~60% of those from the A curve. Operational cycles that add up to 10^8 or more do not come from the kinds of transients normally considered in the evaluation of piping. However, when vibration occurs, the number of cycles can easily add up to $>10^8$.

---

*The proposal includes the formalistic step of changing E from 2.6×10^7 to 2.83×10^7 psi; hence present Code-tabulated stresses for Fig. I-9.2 would be multiplied by 2.83/2.60.

Table B.3. Jaske and O'Donnell design fatigue stresses for high-alloy steels (stresses in ksi)

N	300 Series stainless[a]		Alloy 800[b]		Alloy 600[c]		Combined[d]		Code[e]
	S_a[f]	S'_a[g]	S_a[f]	S'_a[g]	S_a[f]	S'_a[g]	S_a[f]	S'_a[g]	
10	647		644		774		674		708
20	486		466		559		486		512
50	319		309		368		319		345
100	235		230		272		236		261
200	175		174		204		176		201
500	122		124		143		124		148
1000	95.8		99.0		113		97.1		119
2000	77.0		81.3		91.2		78.3		96.9
5000	63.7		65.5		72.1		61.7		76.2
1×10^4	51.9		57.6		62.4		53.3		64.2
2×10^4	45.9		49.5[h]		55.6		47.4		55.5
5×10^4	38.5[h]		38.4[h]		42.8[h]		36.8[h]		46.3
1×10^5	30.2[h]		32.8[h]		36.0[h]		30.8[h]		40.8
2×10^5	25.9[h]		28.8[h]		31.2[h]		26.7[h]		35.9
5×10^5	22.2[h]		25.3[h]		26.9[h]		22.9[h]		31.0
1×10^6	20.3[h]	19.1	23.5[h]		24.8[h]		21.1[h]	20.3	28.3
2×10^6	19.0[h]	17.0	22.3[h]		23.3[h]		19.7[h]	18.1	22.8
5×10^6	17.8[h]	15.3	21.2[h]	20.5	21.9[h]	21.9	18.6[h]	16.3	18.4
1×10^7	17.2[h]	14.5	20.6[h]	19.5	21.2[h]	20.6	18.0[h]	15.5	16.4
2×10^7	16.8[h]	13.9	20.2[h]	18.9	20.8[h]	19.8	17.5[h]	14.9	15.2
5×10^7	16.4[h]	13.4	19.9[h]	18.3	20.3[h]	19.1	17.2[h]	14.4	14.3
1×10^8	16.2[h]	13.2	19.7[h]	18.0	20.1[h]	18.7	17.0[h]	14.1	14.1
1×10^9	15.9[h]	12.8	19.4[h]	17.5	19.8[h]	18.1	16.7[h]	13.7	13.9
1×10^{10}	15.8[h]	12.7	19.3[h]	17.4	19.7[h]	18.0	16.6[h]	13.6	13.7
1×10^{11}	15.8[h]	12.7	19.3[h]	17.4	19.6[h]	17.9	16.5[h]	13.6	13.6

[a] $S = 9{,}081/\sqrt{N} + 31.59$ ksi.

[b] $S = 8{,}557/\sqrt{N} + 38.50$ ksi.

[c] $S = 10{,}393/\sqrt{N} + 39.2$ ksi.

[d] $S = 9{,}058/\sqrt{N} + 33.05$ ksi.

[e] From Table I-9.1 for Fig. I-9.2, multiplied by 28.3/26.0 for E change. For $N > 10^6$, from proposed C curve.

[f] Lesser of S/2 or $S_{a\epsilon}$.

[g] Adjusted for mean stress, Eq. (B.2) with $S_u = 94$ ksi, $S_y = 44$ ksi.

[h] Factor of safety of 2 on stress controls.

Because Jaske and O'Donnell include considerable data in the range of 10^6 to 10^8 cycles and use a more complete set of data than the original Criteria, the use of the proposed A curve appears questionable.

The choice between the B and C curves depends on whether mean stresses will exist. Welds that are not annealed after welding will have yield-strength levels of residual stress. Futhermore, because of installation misalignments, it would be difficult to establish that any part of a piping system is free of mean stress "as installed." Accordingly, it appears that the C curve should be used in piping system fatigue evaluation (e.g., for evaluation of preoperational testing).

Temperature Dependence

The Criteria[1] does not indicate what temperatures were involved in the fatigue tests. However, Langer[3] indicates that tests at temperatures up to 650°F were included for 18-8 stainless steels. Jaske and O'Donnell[2] include tests at temperatures up to 800°F. They converted strains to stresses by using the following room temperature moduli:

300 series stainless steels	28.3×10^6 psi
Alloy 800	27.6×10^6 psi
Alloy 600	31.7×10^6 psi

They used $E = 2.83 \times 10^7$ psi in their combined curve. In principle, the design fatigue curves are temperature dependent because E is temperature dependent.

Jaske[4] presents polished bar, fatigue test data on carbon steel [American Iron and Steel Institute (AISI) 1010], which suggest that fatigue strength increases slightly between 70 and 400°F, then decreases between 400 and 700°F. However, considering the general order of accuracy involved in the fatigue evaluations, it appears appropriate to consider design fatigue stresses for carbon steels to be independent of temperature up to 700°F except as modified by E.

References

1. American Society of Mechanical Engineers, "Criteria of the ASME Boiler and Pressure Vessel Code for Design by Analysis in Sections III and VIII, Division 2," New York, 1969.

2. C. E. Jaske and W. J. O'Donnell, "Fatigue Design Procedure for Pressure Vessel Alloys," *Trans. ASME, J. of Pressure Vessel Technology* 99(4), 584–592 (November 1977).

3. B. F. Langer, "Design of Pressure Vessels for Low-Cycle Fatigue," *ASME Trans, J. Basic Eng.* 84(3), 389–402 (1962).

4. C. E. Jaske, "Low-Cycle Fatigue of AISI 1010 Steel at Temperatures up to 1200F (649C)," *Trans. ASME, J. of Pressure Vessel Technology* 99(3), 432–443 (August 1977).

Appendix C

COMPARISONS OF CARBON STEEL AND AUSTENITIC STAINLESS STEEL PIPING PRODUCT MOMENT FATIGUE TESTS

References 1–5 give results of moment fatigue tests on piping products made of carbon steel and type 304 stainless steel. The tests were similar to Markl's tests[4] in that displacements were controlled. All tests were run on 6-in. nominal size products. Results of these tests are summarized in Table C.1.

Table C.1 contains six sets of comparable results. Because the tests were run at different nominal stress levels, they have been "normalized" by the use of Eq. (9) to obtain i-factors. The fatigue strength, of course, is inversely proportional to the i-factors. The last column shows average ratios, i_c/i_s. If this ratio is <1.00, it means that carbon steel products were stronger than type 304 stainless steel products. It can be seen in Table C.1 that i_c/i_s is <1.00 for all six sets of data.

Table C.2 shows Code 1 carbon steel to stainless steel ratios of fatigue design stresses and the ratios implied by the data in Table C.1. In the region of 10^3 to 10^4 design cycles, the K_e factor adjusts the basic ratios so as to be in better agreement with Table C.1. We have shown the ratios from Table C.1 as applying to $N = 10^3$ and 10^4. Noting that Table C.1 is related to failure cycles N_f, whereas Code 1 data are design cycles N, the ratios from Table C.1 might more appropriately be taken as applying to $N = 10^2$ and 10^3. Also, the Jaske and O'Donnell[5] base data for stainless steel indicate carbon to stainless ratios closer to unity (see Appendix B). However, the anomaly still exists: test data on piping products indicate carbon steel is stronger than stainless steel, whereas Code 1, even with the K_e adjustment, generally indicates the opposite.

While the preceding constitutes the main reason for including this Appendix, the following is a more detailed discussion of Table C.1.

Girth Butt Welds

Markl's tests[4] were on "typical" girth butt welds in 4.5-in.-OD by 0.237-in.-wall pipe. Table C.1 tests were on girth butt welds in 6.625-in.-OD pipe with 0.280-, 0.432-, or 0.718-in.-wall pipe. Details of the welds are not available. That the i-factors are close to unity indicates that Markl's i = 1.0 is rather broadly applicable.

Elbows

The Code 2 i-factor for 6.625-in.-OD by 0.280-in.-wall by 6-in.-bend radius elbows is

$$i = 0.9(r^2/tR)^{2/3} = 0.9(3.1725^2/0.280 \times 6)^{2/3} = 2.97 \ . \qquad (C.1)$$

Table C.1. Comparisons of carbon steel with austenitic stainless steel piping product cyclic moment fatigue tests (data from Refs. 1–3)

Product[a]	Test identity[b]	Material[c]	S_f[d] (ksi)	N_f[e]	i[f]	i_c/i_s[g]
40 Weld	BW-1	C	58.2	35,740	1.03	
	BW-3A	S	61.1	6,950	1.37	0.75
160 Weld	CC-160-1	C	101.6	7,456	0.81	
p = 1050 psi	CS-160-1	S	95.8	7,724	0.85	0.95
80 Weld	BW-15	C	117.6	3,209	0.83	
550°F	BW-14	C	97.3	7,278	0.95	
	BW-12	S	93.8	2,894	1.06	
	BW-11	S	64.2	14,858	1.12	
	BW-10	S	79.0	9,200	1.00	0.84
40 SR Elbow	CCLS-1	C	43.6	1,176	2.73	
p = 1050 psi	CCLS-2	C	42.6	7,899	1.91	
	CSLS-1	S	42.2	6,838	1.99	
	CSLS-2	S	44.2	907	2.84	0.96
40 SR Elbow	HCLS-1	C	43.5	760	2.99	
550°F	HCLS-2	C	43.1	26,100	1.49	
	HSLS-1	S	28.0	2,200	3.75	
	HSLS-2	S	42.2	1,870	2.57	0.71
40 6 x 6 Tee	CCTS-1	C	68.2	21,079	0.98	
	CCTS-2	C	70.6	9,367	1.11	
	CSTS-1	S	68.7	4,575	1.32	
	CSTS-2	S	67.8	3,310	1.43	
	CSTS-3	S	72.7	3,675	1.30	0.77

[a]40 Weld: girth butt weld in sched.-40 pipe; 160 weld: girth butt weld in sched.-160 pipe; 80 Weld: girth butt weld in sched.-80 pipe; 40 SR elbow: sched.-40 short radius (R 6 in.) elbow, 6-in. nominal size; 40 6 x 6 tee: sched.-40 ANSI B19.9 tee, moment through branch. Unless otherwise indicated, tests were run at room temperature with zero internal pressure. Moments were "in-plane" for both elbows and tees.

[b]Identifications used in Refs. 1–3.

[c]C: carbon steel, SA106 Grade B; S: stainless steel, SA312 type 304.

[d]$S_f = M/Z$, M = moment range (completely reversed).

[e]N_f = cycles to failure (through-wall crack).

[f]$i = 490/(S_f N_f^{0.2})$, S_f in ksi [see Eq. (9)].

[g]i_c = average of i's for carbon steel; i_s = average of i's for stainless steel.

Table C.2. Code 1 ratios of fatigue design stresses for carbon steel and austenitic stainless steel

N	Ratios			
	Basic curves[a]	With K_e adjustment[b]		From Table C.1
		$K_s = 1$	$K_s = 2$	
10	0.89	0.60[c]	0.76[c]	
10^2	0.85	0.88[c]	1.05	
10^3	0.76	1.00	0.96	1.04 to 1.41
10^4	0.64	0.91	0.64[d]	1.04 to 1.41
10^5	0.53	0.64[d]	0.53[d]	
10^6	0.48	0.48[d]	0.48[d]	

[a]Ratios obtained from Code 1 Table I-9.1; Fig. I-9.1, UTS $\leq$ 80 ksi for carbon steel; Fig. I-9.2 for austenitic stainless steel.

[b]Ratios are specifically for SA106 Grade B at 100°F to SA312 type 304 at 100°F.

[c]$S_n > 3mS_m$ for one or both materials.

[d]$S_n < 3S_m$ for one or both materials.

Table C.1 indicates that the average value of i is 2.53, about 89% of the value given by Eq. (C.1). This is essentially the same as Markl's in-plane moment results for 4.5-in.-OD by 0.072- or 0.241-in.-wall, 4-in.-bend radius elbows; that is, the experimental i was about 0.85 times the i given by Eq. (C.1). This slight reduction from "theoretical" is deemed to be mainly caused by end effects of the pipes welded to the elbows.

Tees

The Code 2 i-factor for 6.625-in.-OD by 0.280-in.-wall, full outlet ANSI B16.9 tee is

$$i = 0.9(r/4.4t)^{2/3} = 0.9(3.1725/4.4 \times 0.280)^{2/3} = 1.69 \ . \qquad (C.2)$$

Table C.1 indicates that the average value of i is 1.23, about 73% of the value given by Eq. (C.2). Markl's results gave i-factors for in-plane moments ranging from 78 to 109% of i given by Eq. (C.2), the ratio depending on details such as the transition radii and wall thicknesses of the tees.

References

1. J. D. Heald and E. Kiss, "Low Cycle Fatigue of Prototype Pipe Components," General Electric (San Jose) Report GEAP-10763 (January 1973).

2. E. Kiss, J. D. Heald, and D. A. Hale, "Low-Cycle Fatigue of Prototype Piping," General Electric (San Jose) Report GEAP-10135 (January 1970).

3. J. D. Heald and E. Kiss, "Low Cycle Fatigue of Nuclear Pipe Components," *Trans. ASME, J. of Pressure Vessel Technology* 96(3), 171–176 (August 1974).

4. A. R. C. Markl, "Fatigue Tests of Piping Components," *Trans. ASME* 74, 287–303 (1952).

5. C. E. Jaske and W. J. O'Donnell, "Fatigue Design Procedure for Pressure Vessel Alloys," *Trans. ASME, J. of Pressure Vessel Technology* 99(4), 584–592 (November 1977).

NRC FORM 335 (11-81) U.S. NUCLEAR REGULATORY COMMISSION **BIBLIOGRAPHIC DATA SHEET**	1. REPORT NUMBER (Assigned by DDC) NUREG/CR-3243 ORNL/Sub/82-22252/1
4. TITLE AND SUBTITLE (Add Volume No., if appropriate) Comparisons of ASME Code Fatigue Evaluation Methods for Nuclear Class 1 Piping with Class 2 or 3 Piping	2. (Leave blank)
	3. RECIPIENT'S ACCESSION NO.
7. AUTHOR(S) E. C. Rodabaugh	5. DATE REPORT COMPLETED MONTH March YEAR 1983
9. PERFORMING ORGANIZATION NAME AND MAILING ADDRESS (Include Zip Code) E. C. Rodabaugh Associates, Inc. 4625 Cemetery Road Hilliard, Ohio 43026	DATE REPORT ISSUED MONTH YEAR
	6. (Leave blank)
	8. (Leave blank)
12. SPONSORING ORGANIZATION NAME AND MAILING ADDRESS (Include Zip Code) Division of Engineering Technology Office of Nuclear Regulatory Research U.S. Nuclear Regulatory Commission Washington, DC 20555	10. PROJECT/TASK/WORK UNIT NO.
	11. FIN NO. B0474
13. TYPE OF REPORT Topical	PERIOD COVERED (Inclusive dates)
15. SUPPLEMENTARY NOTES	14. (Leave blank)

16. ABSTRACT (200 words or less)

The fatigue evaluation procedure used in the ASME Boiler and Pressure Vessel Code, Section III, Nuclear Power Plant Components, for Class 1 piping is different from the procedure used for Class 2 or 3 piping. The basis for each procedure is described and correlations between the two procedures are presented. Conditions under which either procedure, or both, may be unconservative are noted.

Potential changes in the Class 2 or 3 piping procedure to explicitly cover all loadings are discussed. However, the report is intended to be informatory and, while the contents of the report may guide future Code changes, specific recommendations are not given herein.

17. KEY WORDS AND DOCUMENT ANALYSIS

17a. DESCRIPTORS

17b. IDENTIFIERS OPEN-ENDED TERMS

18. AVAILABILITY STATEMENT	19. SECURITY CLASS (This report)	21. NO. OF PAGES
Unlimited	Unclassified	
	20. SECURITY CLASS (This page) Unclassified	22. PRICE $

NRC FORM 335 (11-81)

9511160312